EurJOC European Journal of Organic Chemistry

FULL PAPER

DOI: 10.1002/ejoc.201200159

A Joint Experimental and Computational Investigation on Homoconjugated Push-Pull Chromophores Derived from 7,7-Diphenylnorbornane

Noelia Herrero-García,[a] María del Rosario Colorado Heras,[a] María del Rosario Torres,[b] Israel Fernández,*[a] and José Osío Barcina*[a]

Keywords: Donor-acceptor systems / Homoconjugation / Charge transfer / DFT calculations / Transannular interactions

We report hereon the synthesis, spectroscopic properties and computational studies of novel aromatic homoconjugated compounds derived from 7,7-diphenylnorbornane (DPN). The UV/Vis spectra of these compounds show bands corresponding to the respective chromophores as well as new homoconjugation bands and charge transfer absorptions in D–DPN–A push-pull derivatives. Homoconjugation between the aromatic rings strongly depends on the nature of the substitution at the aryl moieties. Therefore, electronic communication by homoconjugation can be easily tuned by controlling the electronic nature and positions of the substituents. The strong homoconjugative interaction is also reflected in the reactivity, NMR spectra and NLO properties of the compounds studied. DFT calculations nicely agree with the experimental data and shed light on the electronic delocalization via homoconjugation.

Introduction

Over the past years a considerable effort has been devoted on the design, synthesis and study of the properties of conjugated push-pull molecular chromophores (D–π–A) and their oligomeric and polymeric derivatives.[1–5] Interest in such systems is justified by their important technological applications in molecular electronics and optoelectronics[6] as e.g. nonlinear optical (NLO) materials,[6,7] molecular wires,[8] solvatochromic probes,[9] or organic photorefractives.[10]

Recently, several strategies have been developed in order to modulate the properties (HOMO–LUMO gap, solubility, processability) of push-pull systems. Thus, nonplanar D–π–A chromophores have been reported and the influence of nonplanarity on their conjugative properties has been investigated (**1**, Figure 1).[11–13] A different approach involves the use of bridges between the donor and acceptor groups with non-conventional electron delocalization, as in compounds **2** with cross-conjugated bridges,[14] spiro systems **3**,[15] and also compounds with saturated bicyclic connectors.[16] At this respect, aromatic homoconjugated systems have received little attention. Examples of lateral homoconjugated push-pull systems derived from triptycene have been reported.[17,18] However, electron delocalization by homoconjugation in iptycenes such as triptycene is not clear and remains controversial.[19] Very recently, homoconjugated push-pull systems obtained by [2+2] cycloaddition reaction between 2,3-dichloro-5,6-dicyano-1,4-benzoquinone (DDQ) and *N*,*N*-dialkylanilino (DAA) (**4**, Figure 1) or ferrocene-substituted alkynes have been described.[20] The resulting D–A chromophores show strong intramolecular CT interactions and promising third-order nonlinear optical properties.

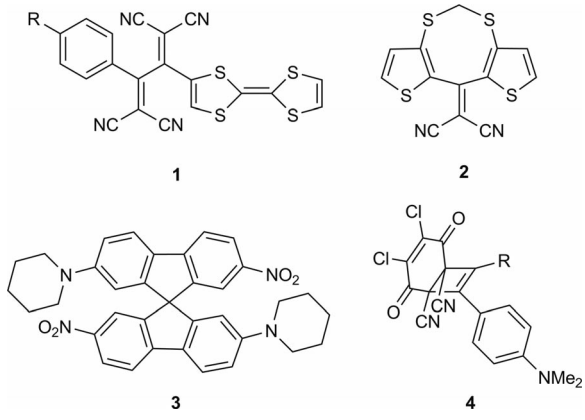

Figure 1. Examples of nonplanar, cross-conjugated, spiro, and homoconjugated push-pull chromophores **1**–**4**, respectively.

Aromatic apical homoconjugated compounds derived from 7,7-diphenylnorbornane (DPN) (**5c**, Figure 2) are a family of interesting derivatives featuring non-conventional electron delocalization within the cofacially arranged aryl groups.[21–26] Homoconjugated push-pull systems were synthesized and used for the first time to study the nature of

[a] Departamento de Química Orgánica, Facultad de Ciencias Químicas, Universidad Complutense de Madrid, Ciudad Universitaria s/n, 28040 Madrid, Spain
Fax: +34-91-3944103
E-mail: israel@quim.ucm.es
josio@quim.ucm.es
[b] Laboratorio de Difracción de Rayos X, Facultad de Ciencias Químicas, Universidad Complutense de Madrid, Ciudad Universitaria s/n, 28040 Madrid, Spain
Supporting information for this article is available on the WWW under http://dx.doi.org/10.1002/ejoc.201200159.

 © 2012 Wiley-VCH Verlag GmbH & Co. KGaA, Weinheim

face to face aromatic interactions.[21] Further studies demonstrated that these compounds show remarkable second-order NLO properties, with β_z(1064 nm) values comparable to those measured for linearly conjugated analogous.[22] More recently, the first example of efficient photoinduced energy transfer mediated by an homoconjugated bridge in the heterodinuclear D–B–A complex $[Ru–DPN–Ir]^{3+}$ has been reported.[23]

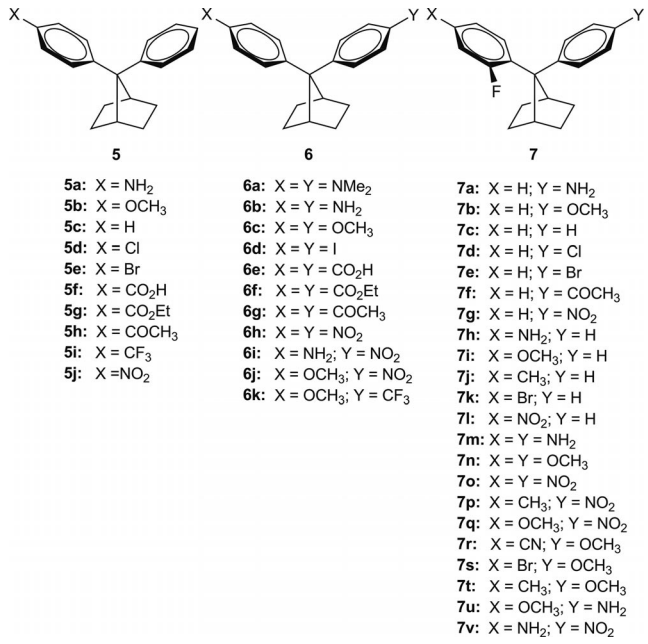

Figure 2. Mono- and disubstituted derivatives of DPN and FDPN **5**–**7**.

In previous works we have studied electron delocalization in DPN as well as in derived polymers[24] and oligomers[25] by absorption spectroscopy and TD-DFT calculations.[26] The results of these investigations confirm that aromatic homoconjugation in acyclic systems is an effective mechanism for electron delocalization with an effective homoconjugation length for homoconjugated oligomers of 6–7 aryl rings. Our previous calculations also pointed out the importance of transannular interactions in push-pull systems derived from DPN. Now, in order to check this hypothesis and provide further information on electron delocalization in these aromatic homoconjugated systems, we have performed an extensive joint computational-experimental study in substituted DPNs, with special emphasis on push-pull DPN derivatives. The electronic communication between the donor and acceptor moieties has been studied by UV/Vis and NMR spectroscopy. The experimental results were correlated with DFT and TD-DFT calculations.

Computational Details

Geometry optimizations without symmetry constraints were carried out using the Gaussian09 suite of programs[27] at the dispersion corrected meta-hybrid functional M06–2X functional[28] in combination with the standard double-ζ plus polarization 6-31+G(d) basis sets.[29] Stationary points were characterized as minima by calculating the Hessian matrix analytically at this level. Calculations of absorption spectra were accomplished by using the time-dependent density functional theory (TD-DFT)[30] method. The assignment of the excitation energies to the experimental bands was performed on the basis of the energy values and oscillator strengths. The B3LYP[31] Hamiltonian was chosen because it was proven to provide reasonable UV/Vis spectra for a variety of chromophores[26,32] including organometallic species.[33] Total first hyperpolarizabilities (β_{tot}) were computed according to the following equation using the different β_{ijk} tensor components:

$$\beta_{tot} = sqrt\left[\left(\beta_{xxx} + \beta_{xyy} + \beta_{xzz}\right)^2 + \left(\beta_{yyy} + \beta_{yzz} + \beta_{yxx}\right)^2 + \left(\beta_{zzz} + \beta_{zxx} + \beta_{zyy}\right)^2\right]$$

Results and Discussion

Synthesis and Structure of DPNs

For this study we have chosen the series of mono- and disubstituted derivatives of DPN (**5** and **6**) and 7-(*o*-fluorophenyl)-7-phenylnorbornane (FDPN, **7**) depicted in Figure 2. The synthesis of these compounds was carried out according to the methodology described previously by us (Scheme 1).[21–26] One of the advantages of DPNs is that a large variety of different molecules can be prepared following standard and straightforward procedures. Electrophilic aromatic substitution reactions on both DPN and FDPN take place exclusively at the *para* position, since the *ortho* position is sterically hindered by the bridgehead hydrogen atom of norbornane. The only exception to this behaviour was found while attempting the synthesis of **7o**, the FDPN derivative with two *para* nitro groups as substituents (Scheme 2). While nitration reaction of DPN yields the corresponding dinitro derivative **6h** in high yield, reaction of **7c** under the same conditions yields a 25:75 mixture of **7o** and **8** (Scheme 2). Since these compounds are difficult to separate, the synthesis of **7o** was carried out by nitration of the mononitro derivative **7l**.[21]

The formation of the *meta*-substituted compound **8** can be explained considering that, in the first step of the nitration reaction, **7g** is obtained as the main reaction product due to the deactivating effect of the fluorine atom (Scheme 2). In the second step, electrophilic aromatic substitution takes place at the *meta* position of the fluorinated ring induced by both the deactivating effects of fluorine and the nitro group of the adjacent homoconjugated aromatic ring. Moreover, nitration of **7g** affords compound **8** in 86% yield. This fact, together with the experimental observation that reaction rate of the second nitration reaction is lower than the first nitration, is a clear evidence of strong transannular homoconjugative interaction in DPNs, similar to that observed in cyclophanes.[34–36] In a previous work we have shown that DPNs can be considered as examples of "open-chain cyclophanes" (protophanes).[24b]

 © 2012 Wiley-VCH Verlag GmbH & Co. KGaA, Weinheim

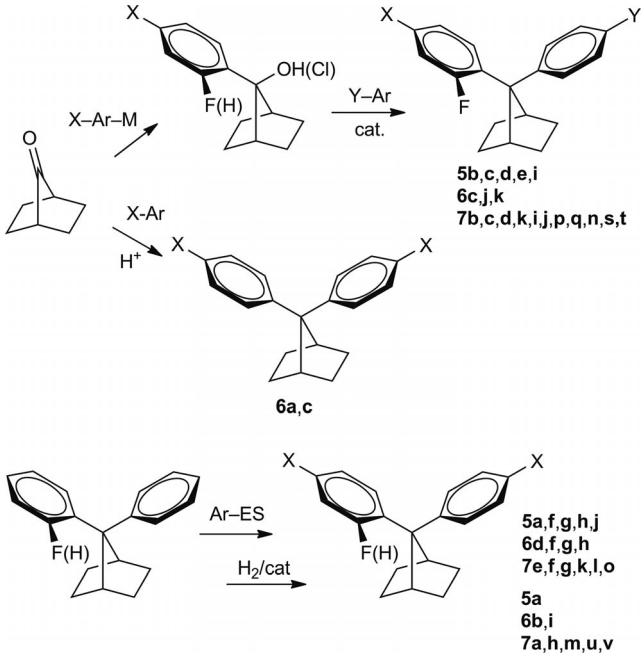

Scheme 1. General synthetic routes for DPN and FDPN derivatives.

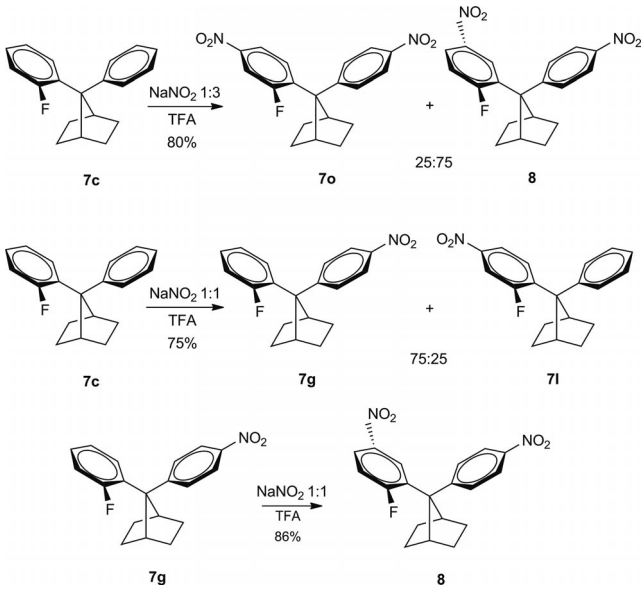

Scheme 2. Synthesis of nitro derivatives of FDPN.

Compounds **9a**–**e** derived from 2,2-diphenylpropane and **10b**–**c** have been prepared as references for the study of the spectroscopic properties of DPNs (Figure 3). It should be noted that in **10a**–**c**, the most stable conformation is the orthogonal disposition, since the aryl rings cannot adopt the cofacial conformation because of the restricted mobility of the fused phenyl ring. Therefore, homoconjugative interactions are not expected in these derivatives. On the other hand, the most stable conformation of 2,2-diphenylpropanes is the helicoidal conformation. The synthesis of these compounds was carried out following the same procedures used for the analogous DPNs starting from the 2,2-diphenylpropane and bicyclic compound **10a** (see Supporting Information).

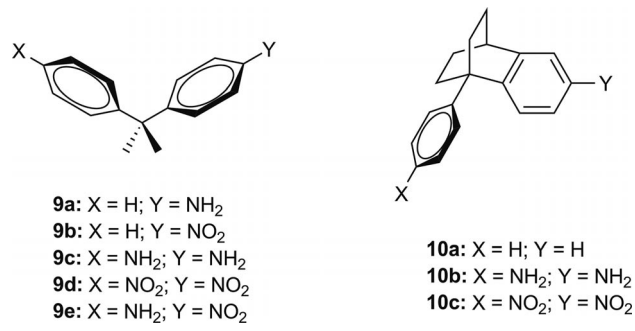

Figure 3. Structures of reference compounds **9** and **10**.

The main structural features of the compounds described in this work are highlighted by the push-pull system **6i**. The crystal structure of **6i** (Figure 4) confirms the characteristic cofacial arrangement of the aryl groups in DPNs. Thus, the values of the C15–C14–C7–C8 and C9–C8–C7–C14 torsion angles are 92.3 and 89.1° respectively. On the other hand, the value of the C14–C7–C8 bond angle is 107.8° and the distance between the *ipso* carbon atoms of the aryl rings (C14–C8), 2.468 Å, well below the sum of the van der Waals radii for two phenyl rings (3.4 Å).[37a]

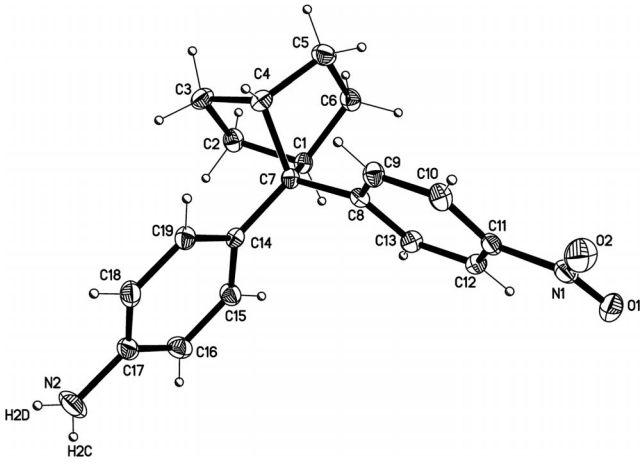

Figure 4. X-ray crystal structure of compound **6i**.

The crystal packing of **6i** (Figure 5) shows some remarkable features. It has been described that nitroanilines crystallize into predictable arrays forming intramolecular hydrogen bonds between the amino and nitro groups. These interactions occur so frequently that can be used to establish hydrogen bond rules which are useful tools to predict and design crystalline materials.[38] However, no nitro···amino hydrogen bonds are detected in the case of **6i**. Instead, short amino···amino contacts are observed. The H2C atom of the amino group interacts with the N2' of the neighbouring molecule: H2C···N2′ distance of 2.614 Å, with N2–H2C–N2′ angle of 144.6° and distance between

 © 2012 Wiley-VCH Verlag GmbH & Co. KGaA, Weinheim

N2 and N2′ amino N atoms, 3.352 Å. The shorter distance between amino and nitro groups is observed in the case of H2D and O1 (2.994 Å). On the other hand, short contacts are detected between the nitro oxygen atoms and H10 and H18 hydrogen atoms of the neighbouring aryl rings of two different molecules (O2···H10 2.597 Å; O1···H18 2.618 Å). On the basis of distance criteria, the interaction between the amino groups can be considered as hydrogen bond since the distance (2.614 Å) is shorter than the sum of the van der Waals radii of hydrogen and nitrogen atoms (1.10 Å and 1.55 Å, respectively).[37b]

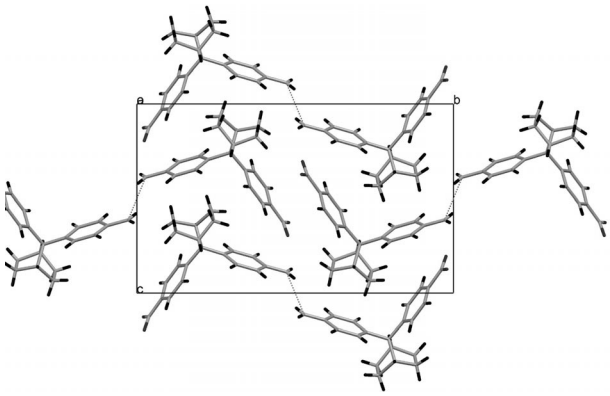

Figure 5. Crystal packing of **6i** showing the amino···amino short contacts.

Absorption Spectroscopy Study

Absorption spectroscopy constitutes an appropriate method to study electron delocalization and transannular interactions in aromatic systems. In previous works we have used UV/Vis spectra to study electron delocalization in homoconjugated DPNs[26] as well as oligomers[25] and polymers[24] derived from DPN. These studies clearly show that aromatic homoconjugation is an effective mechanism for electron delocalization that resembles the situation described for polyphenylenes. We have also performed TD-DFT calculations on these systems,[26] finding a good agreement between the TD-DFT-computed lowest energy vertical transitions and the experimentally observed absorptions. Therefore, TD-DFT calculations can be used to accurately assign the vertical transitions responsible for the observed spectra in homoconjugated DPNs.

The UV/Vis spectra of DPNs and FDPNs show three important absorption bands: a) the bands of the corresponding chromophores attached to the aryl rings, b) the new homoconjugation bands, and c) charge-transfer bands in push-pull systems with strong electron-withdrawing and electron-donating groups in their structures. Tables 1, 2, and 3 show the wavelengths of the absorption maxima of the bands for all compounds studied in this work. For those cases where the band appeared as a shoulder, the position of these absorptions has been established by the derivative method.

Table 1. Absorption spectra (λ_{max}, MeOH) of monosubstituted DPNs and FDPNs.

	λ [nm] ε ($M^{-1}cm^{-1}$)		λ [nm] ε ($M^{-1}cm^{-1}$)		λ [nm] ε ($M^{-1}cm^{-1}$)
5a	249 (13800)[a]	**5i**	233 (11600)	**7f**	259 (16000)
5b	238 (13800)[a]	**5j**	289 (10000)	**7g**	284 (11800)
5c	229 (13300)[a]	**7a**	249 (10300)[a]	**7h**	246 (10400)[a]
5d	234 (13600)[a]	**7b**	234 (15100)[a]	**7i**	234 (14700)[a]
5e	236 (12800)[a]	**7c**	226 (12300)[a]	**7j**	229 (13700)[a]
5f	250 (15000)	**7d**	232 (16000)[a]	**7k**	234 (16100)[a]
5g	250 (11800)	**7e**	232 (20200)[a]	**7l**	285 (11800)
5h	262 (15200)				

[a] Homoconjugation band.

Table 2. Absorption spectra (MeOH) of disubstituted DPNs and FDPNs with X = Y groups.

	λ [nm] ε ($M^{-1}cm^{-1}$)		λ [nm] ε ($M^{-1}cm^{-1}$)
6a	259[b], 272 (20000)[a]	**6g**	248 (20700), 269 (28400)
6b	234 (12700), 255 (18600)[a]	**6h**	284 (16900)
6c	242 (18300)[a]	**7m**	237,[b] 253 (12100)[a]
6d	230 (7000), 247 (11300)[a]	**7n**	239 (16900)[a]
6e	234 (10400), 256 (15000)	**7o**	273 (11900)
6f	235 (17400), 258 (26700)		

[a] Homoconjugation band. [b] Shoulder.

The influence of electron delocalization by homoconjugation is revealed by the bathocromic shift of the chromophores' bands in comparison to the corresponding spectra of benzene derivatives:[39] compounds **5f** (250 nm) and **6e** (256 nm) and benzoic acid (226 nm); **5g** (250 nm) and **6f** (258 nm) and etoxycarbonylbenzene (228 nm); **5h** (262 nm), **7f** (259 nm) and **6g** (269 nm) and acetophenone (242 nm); **5i** (233 nm) and trifluoromethylbenzene (210 nm); **5j** (289 nm), **7g** (284 nm), **7l** (285 nm) and **6h** (284 nm) and nitrobenzene (251 nm). Furthermore, the position of the band depends on the effect of the substituent placed on the adjacent ring. This effect is similar to the transannular interaction described for cyclophanes.[34–36] Thus, in the series of nitro derivatives **5j**, **6h**, **6i**, **6j** (DPN), **7g**, **7l**, **7o**, **7p** and **7q** (FDPN) there is a correlation between the wavelength of the absorption band of the nitro groups and the corresponding Hammett substituent constant σ_p[40] of the substituent placed at the opposite aryl ring. Figure 6 shows the absorption spectra of compounds **7g**, **7o**, **7p** and **7q** as well as the linear relationship between the wavelengths of the absorption maxima of the nitro group and the nature of the substituents placed at the adjacent aryl ring according to their σ_p value. A similar situation is observed with the analogous DPN derivatives.

Gas-phase TD-DFT calculations on compounds **7g**, **7o**,**p**,**q** also show the presence of two main absorptions. The band around 300 nm (which is slightly redshifted in the calculations due to solvatochromism) is ascribed in all cases to the promotion of one-electron from the HOMO to the LUMO. As expected, both frontier orbitals are π molecular orbitals, thus indicating the π-π* nature of this absorption. Inspection of the involved orbitals reveals that the HOMO is mainly centered in the flouroaryl moiety whereas the LUMO is centered in the adjacent *p*-NO_2-aryl group (Fig-

 © 2012 Wiley-VCH Verlag GmbH & Co. KGaA, Weinheim

Table 3. Absorption spectra (MeOH) of disubstituted DPNs and FDPNs with X ≠ Y groups.

	λ [nm] ε ($M^{-1}cm^{-1}$)		λ [nm] ε ($M^{-1}cm^{-1}$)
6i	247 (13200), 293 (9800), 320[b,c]	**7r**	225 (12300),[a] 268 (7600), 288[b,c]
6j	227 (12250),[a] 277 (8100), 303[b,c]	**7s**	242 (16500),[a] 270 (6900)
6k	247 (9800),[a] 260–290[c,d]	**7t**	237 (14300)[a]
7p	286 (7800), 275–340[c,d]	**7u**	224,[b] 247 (12000)[a]
7q	223 (14500),[a] 281 (7800),[c,d] 288 (7600)	**7v**	250 (9300), 250–425[c,d]

[a] Homoconjugation band. [b] Shoulder. [c] Charge transfer band. [d] Overlapping bands.

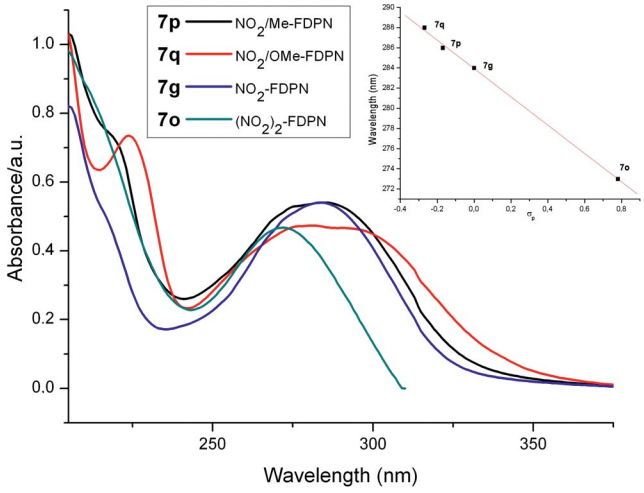

Figure 6. Absorption spectra of NO_2-substituted FDPN and correlation between the absorption wavelength and the σ_p value of the substituent placed on the adjacent homoconjugated ring.

ure 7). For this reason, it is not surprising that a more effective charge transfer (i.e. a redshift) occurs with better π-donors attached to the *para*-position of the fluoro-aryl fragment in agreement with the above-mentioned Hammett plot. Moreover, the band around 230 nm is ascribed to the HOMO–3 to LUMO transition by our TD-DFT calculations. As seen in Figure 7, the HOMO–3 is a delocalized orbital between both aryl substituents thus confirming the homoconjugated nature[26] of this absorption.

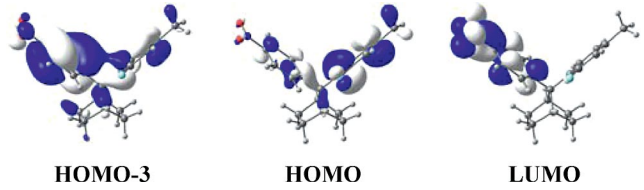

Figure 7. Computed molecular orbitals of compound **7p** (isosurface value of 0.03 au).

In the case of amino-substituted DPNs and FDPNs, the absorption band of the chromophore appears overlapped with the homoconjugation bands in most of the derivatives and can be observed only in compounds where the homoconjugation band is redshifted (vide infra). In these compounds, a similar behaviour is observed: i.e. the absorption band is redshifted in going from compound to **7u** (224 nm) to **7m** (237 nm).

Finally, the effect of homoconjugation in DPNs can be also observed by comparison of the absorption wavelength of the nitro derivatives **5j** (289 nm) and **6h** (284 nm) with the analogous 2,2-diphenylpropanes **9b** and **9d** (276 nm). Similarly, TD-DFT calculations assign this band (for **5j**) to a combination of the HOMO–3 and HOMO–2 to LUMO vertical transitions (calculated excitation energy of 270 nm). The shape of these π-molecular orbitals resembles that of HOMO–3 (**7p**), confirming the delocalization of electrons in both aryl moieties due to homoconjugation (see Supporting Information).

One of the most relevant features of the compounds studied in this work is related to the homoconjugation band. We have previously described that DPN shows a characteristic homoconjugation band at 229 nm. The position of this absorption depends on the torsion angle of the aryl rings and the extension of the homoconjugation. Thus, deviations from the cofacial conformation cause hypsochromic shifts of the band. On the other hand, a bathochromic shift is observed in DPN oligomers because of the extension of the homoconjugation.[25,26]

In the substituted DPNs studied herein, the nature of the substituents on the aryl rings exerts a very important effect on the electron delocalization between the aromatic rings. Thus, electron-withdrawing groups diminish the electron density and, consequently, the homoconjugative effect is almost imperceptible, as revealed by the hypsochromic shift of the homoconjugation band with e.g. nitro-substituted DPNs and FDPNs **5j**, **6h**, **7g**, **7l** and **7o**. In contrast, electron-donating groups show the opposite effect, as they increase the electron density and consequently the homoconjugation between the aryl rings. This is observed with methyl-, methoxy- and amino-substituted DPNs and FDPNs **5a**, **5b**, **6a**, **6b**, **6c**, **7a**, **7b**, **7h**, **7i**, **7j**, **7m** and **7n** in which bathochromic shifts of the corresponding homoconjugation bands are observed (see Tables 1, 2, and 3). The only exception to this behaviour was found in halogen-substituted DPNs and FDPNs **5d**, **5e**, **6d**, **7d**, **7e** and **7k**. The homoconjugation band in these derivatives is redshifted, pointing to a predominance of the conjugative effect of these atoms on the wavelength of the homoconjugation band, as observed in the absorption bands of halogen substituted benzenes.[39] Strikingly, the homoconjugation band of FDPN (**7c**) is blueshifted in comparison with the band of DPN (**5c**). The reasons for this differential behaviour can be found in the inductive effect of the fluorine atom at the *ortho* position (which is in part responsible for the observed hypsochromic shift of FDPN)[39] and the influence

 © 2012 Wiley-VCH Verlag GmbH & Co. KGaA, Weinheim

of this atom on the cofaciallity of the aryl rings (which would diminish the homoconjugation between the aryl rings).[26]

The substituents effect on the communication between the aryl groups in homoconjugated derivatives is clearly revealed by comparison with the UV/Vis spectra of the orthogonal chromophores **10b** and **10c**. As mentioned above, electron-releasing groups such as NO_2 diminish the electron density between the aromatic rings and, consequently, homoconjugation is less effective. The absorption spectra of **10c** shows an absorption maximum at 276 nm, the same wavelength observed for the diphenylpropane derivatives **9b** and **9d**. These bands are characteristic of aromatic nitro derivatives. The spectra of **5j** (289 nm), **6h** (284 nm) and **7o** (273 nm) are quite similar, showing the effect of delocalization by homoconjugation and the deviation from the cofacial conformation in the case of **7o**. The homoconjugation band in these compounds is blueshifted by the NO_2 groups and is difficult to observe. Interestingly, the situation observed for the amino derivatives is remarkably different. The absorption spectra of the diamino orthogonal derivative **10b** resembles that of aniline, showing an intense strong band at 239 nm (230 nm in aniline) and a weak absorption (^1L_b band) at 285 nm (281 nm in aniline) (Figure 8). The spectra of diphenylpropane derivatives **9a** (238 and 289 nm) and **9c** (241 and 289 nm) are similar. While the homoconjugation bands are not observed in these compounds, the spectra of **6b** and **7m** are dominated by the homoconjugation bands at 255 and 253 nm, respectively. Moreover, the homoconjugation band is redshifted up to 272 nm in the case of compound **6a**, in agreement with the higher electron-donating nature of the NMe_2 group. These results demonstrate that communication by homoconjugation between aromatic moieties can be easily tuned by controlling the electronic nature of the substituents attached at the aryl rings. Interestingly, our TD-DFT calculations assign the homoconjugation band in **6b** to the HOMO→LUMO+1 vertical transition (λ_{calc} = 262 nm). Figure 9 nicely shows that this virtual orbital is delocalized between both aryl moieties thus confirming the electronic communication in this species. As expected, no similar delocalized orbital can be found in the non-cofacial analogue **10b**. This provokes that both aryl groups are electronically isolated and therefore, this species behaves quite similarly to aniline.

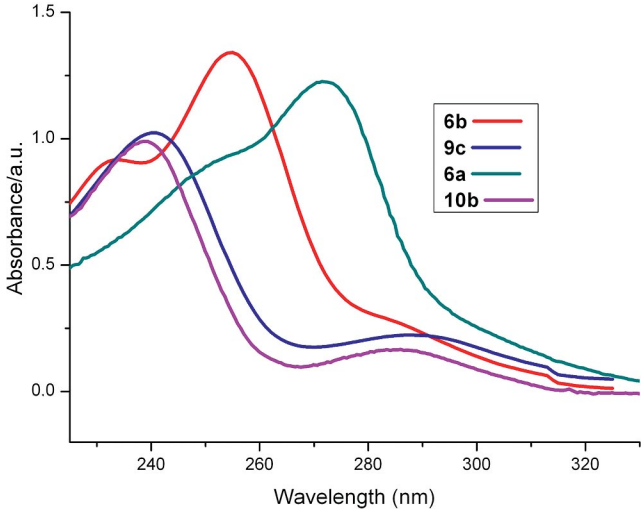

Figure 8. Absorption spectra of amino-substituted compounds.

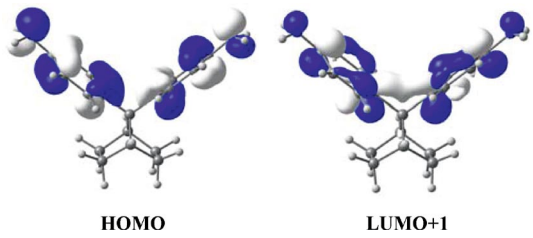

Figure 9. Computed molecular orbitals of compound **6b** (isosurface value of 0.035 au).

The position of the homoconjugation bands strongly depends on the nature of the substituents. Figure 10 shows the absorption spectra of MeO-FDPNs with different substituents on the homoconjugated aromatic ring. As can be seen, there is an excellent correlation (r^2 = –0.996) between the position of the homoconjugation band and the σ_p value of the respective group. Only the bromo derivative **7s** deviates from this behaviour, as observed before for the halogen-substituted DPNs and FDPNs (vide supra). The same behaviour is observed for the MeO-DPNs **5b**, **6c**, **6j** and **6k** as well as in the series **5a–c**, **6a–c, 7a–c**, **7h–j** and **7m–n**.

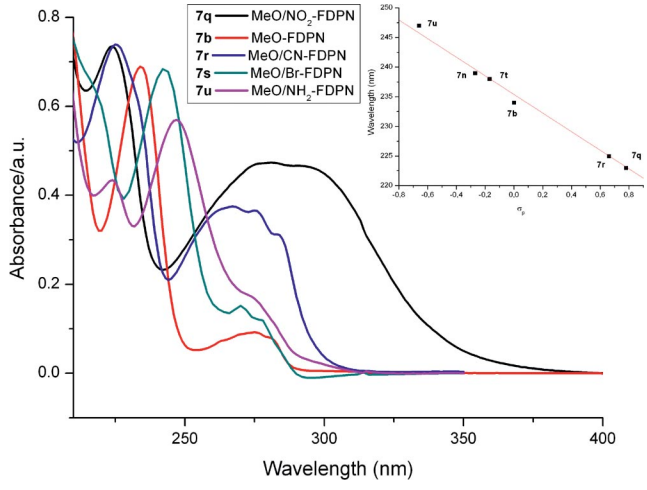

Figure 10. Absorption spectra of MeO-substituted FDPN and correlation between the absorption wavelength and the σ_p value of the substituent placed on the adjacent ring. The absorption spectra of **7n** and **7t** are omitted for clarity.

The situation observed in push-pull DPNs with strong electron-donating and releasing groups is particularly interesting. When both electron-withdrawing and -donating substituents are placed at the *para* positions, besides the chromophore and homoconjugation absorptions, charge-transfer bands are observed in the corresponding UV/Vis spectra of compounds **6i**, **6j**, **6k**, **7p**, **7q**, **7r** and **7v** (Table 3).

 © 2012 Wiley-VCH Verlag GmbH & Co. KGaA, Weinheim

The absorption spectra of compounds **6j**, **6k**, **7p**, **7q** and **7r** are shown in Figure 11. Compounds **6j** and **7q** show broad absorptions corresponding to two overlapping bands between 250–375 nm. These bands are the sum of the charge-transfer band and the nitro group absorption. A similar situation is observed in **7p**, although in this case a narrower band is observed, in accordance with the less donating character of the methyl group. In the case of compound **7r**, the charge-transfer band is observed between 250–300 nm and in **6k** the residual absorption at longer wavelength can be assigned to the charge-transfer band (see supplementary material). The cut-off of the CT bands in compounds **6j**, **7p** and **7q** lies between 380–390 nm.

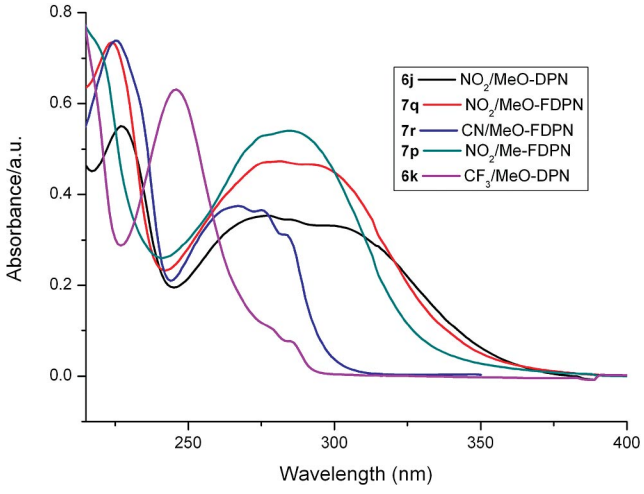

Figure 11. Absorption spectra of compounds **6j**, **6k**, **7p**, **7q** and **7r** showing the charge-transfer bands.

Figure 12 shows the absorption spectra of compound **6i**, **7v** and the analogous 2,2-diphenylpropane derivative **9e**. Comparison of these spectra reveals the presence of a charge-transfer band between 300–450 nm in **6i**. This band is not observed or is much less pronounced in **9e** (cut-off: 385 nm). The spectrum of **7v** shows a broad absorption band, sum of the NH_2, NO_2 chromophores and the CT band, with a maximum at 250 nm and cut-off ca. 425 nm. Previous studies carried out on diphenylmethane and 2,2-diphenylpropane with nitro and amino groups as substituents describe the presence of a weak charge-transfer band as the tail of the long wavelength band of the nitro group.[41] These results nicely illustrate the remarkable effect of homoconjugation in our compounds. In fact, this effect is just the consequence of the imposed geometry by the DPN fragment which places both aromatic rings in a cofacial orientation allowing for the observed charge transfer. Obviously, this geometrical constrain is not present in the analogous derivative **9e** or orthogonal chromophores **10** (see Figure 13) and therefore, there is no chance for the electrons to delocalize by homoconjugation.

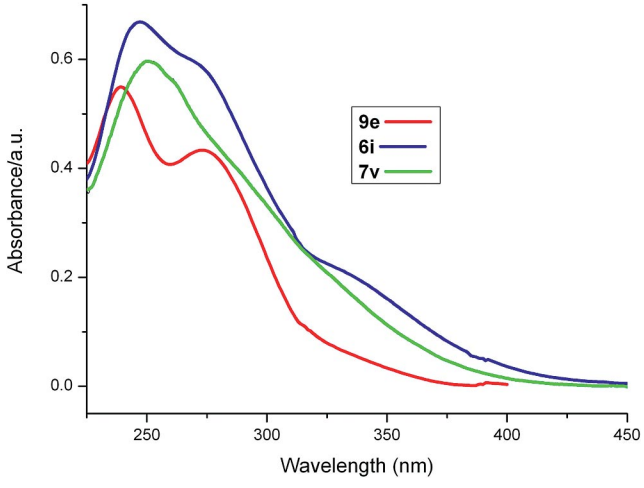

Figure 12. Absorption spectra of compounds **6i** and **9e**.

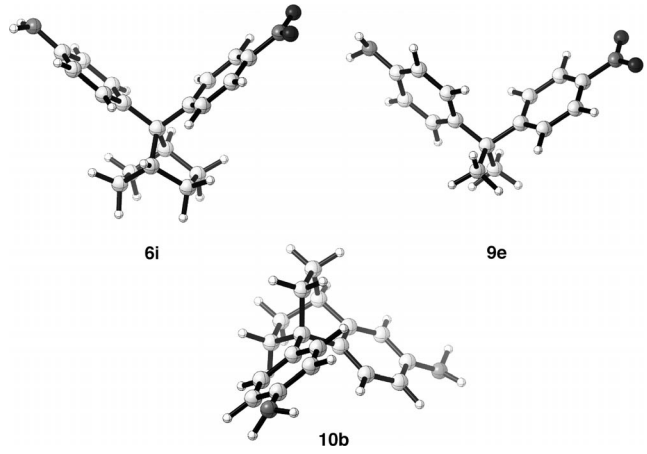

Figure 13. Fully optimized geometries (M06-2X/def2-SVP level) of compounds **6i** and **9e** and **10b**.

Comparison of the absorption spectra of **6i** with the *meta* substituted analogous FDPN leads to some significant conclusions. Partial hydrogenation of **8** (Scheme 3) produces a mixture of *meta*-substituted nitro/amino derivatives **11** and **12**. In the UV/Vis spectra of these compounds (**11**: λ_{max} = 283 nm; **12**: λ_{max} = 263 nm) no CT band are observed (see Supporting Information), showing that charge transfer from the donor to the acceptor groups is favoured by sub-

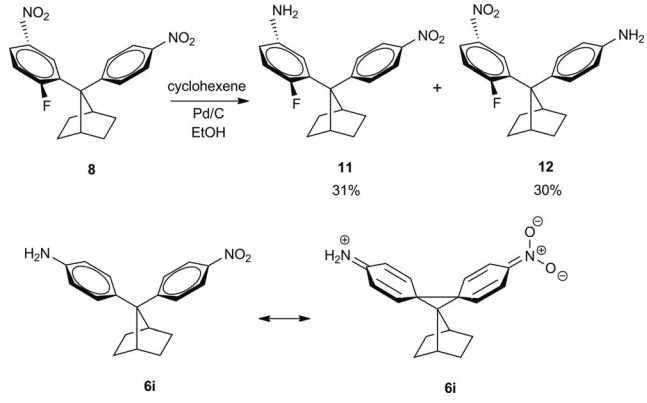

Scheme 3. Synthesis of *meta* FDPNs **11** and **12** and resonance structures of push-pull derivative **6i**.

 © 2012 Wiley-VCH Verlag GmbH & Co. KGaA, Weinheim

stituents placed at the *para* positions of the aromatic rings. In this regioisomer, the homoconjugative interaction reaches its maximum, according to the homoconjugated resonance structure of **6i** depicted in Scheme 3.

NLO Properties

In a previous work we described the first study reported to date on the NLO properties of homoconjugated compounds.[22] Our results show that push-pull systems derived from DPN and FDPN present significant SHG hyperpolarizabilities. The values of β_z value measured for our DPNs and FDPNs are higher than the obtained for non-homoconjugated analogous and comparable to conjugated push-pull systems. Thus, the β_z(1064 nm) value measured for compound **6i** was 21×10^{-30} esu, three times higher than the observed for **9e** and equal to the measured for *p*-nitroaniline under the same experimental conditions.

Herein we have computed the total first hyperpolarizability (β_{tot}) values of different nitro-substituted DPNs and FDPNs (Table 4). As expected, the computed β_{tot} values are generally higher in DPNs than in their FDPNs counterparts. This is mainly due to the effect of the fluorine atom at the *ortho* position, which slightly modifies the cofacial orientation, leading to a less effective homoconjugation. Interestingly, push-pull systems exhibit higher β_{tot} values than compounds possessing an electron-withdrawing group at the aryl group adjacent to the *p*-NO_2-aryl fragment. Moreover, the β_{tot} computed for the NH_2 systems is comparable to the β_{tot} value obtained for truly π-conjugated push-pull systems,[42] thus indicating that homoconjugation can be indeed as effective in communicating the donor and acceptor moieties in our DPNs (or FDPNs) as π conjugation. Not surprisingly, nice linear relationships were obtained when plotting the computed β_{tot} values vs. the corresponding Hammett substituent constant σ_ps (Figure 14, correlation coefficient r^2, of –0.995 and –0.986 for DPNs and FDPNs, respectively) as a consequence of the higher homoconjugation occurring with better π-donor groups.

Table 4. Computed β_{tot} (B3LYP/def2-SVP//M06-2x/def2-SVP level) for different DPNs and FDPNs.

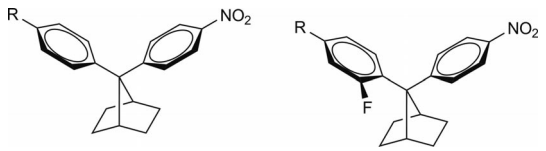

R	β_{tot} /10^{-30} esu	β_{tot} /10^{-30} esu
NH_2	29.85	23.70
OCH_3	23.77	19.50
Br	15.20	12.67
CN	9.67	9.24
NO_2	9.37	9.84

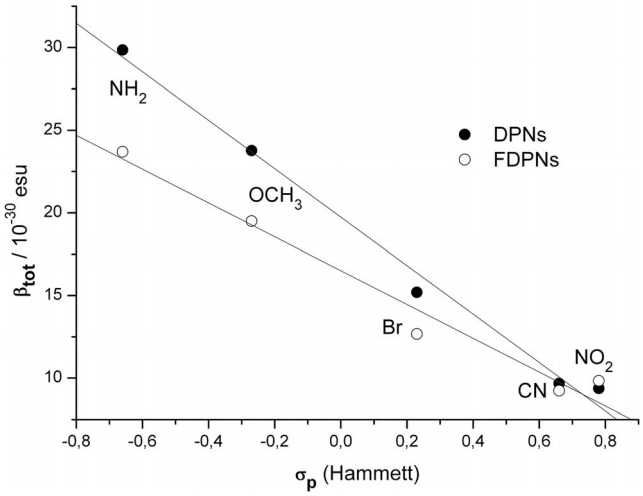

Figure 14. Plots of β_{tot} vs. σ_p substituent constants.

NMR Spectroscopy

To complete this study, we have also checked the influence of homoconjugation in DPNs and FDPNs by NMR spectroscopy. The chemical shifts of the most significant protons and carbon atoms of the compounds studied are listed in Table 5. These data show that the effect of a certain group in one of the aryl rings is transferred to the adjacent ring by means of homoconjugation. In Figure 15, the varia-

Table 5. Selected ^{1}H NMR and ^{13}CNMR spectroscopic data (δ, ppm, $CDCl_3$) of DPNs and FDPNs.

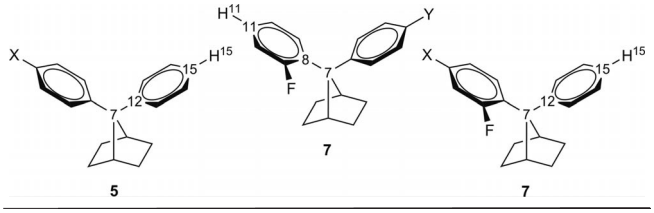

	δ_{H15}	δ_{C7}	δ_{C8}	δ_{C11}	δ_{C12}	δ_{C15}
5a	7.04	63.95	–		146.63	125.01
5b	7.06	64.04	–	–	146.37	125.18
5c	7.07	64.79	–	–	145.97	125.29
5d	7.09	64.38	–	–	145.45	125.57
5e	7.07	64.44	–	–	145.34	125.58
5f	7.09	65.16	–	–	144.87	125.77
5g	7.09	64.85	–	–	144.94	125.75
5h	7.09	65.08	–	–	144.86	125.75
5i	7.11	64.91	–	–	144.96	125.79
5j	7.12	65.04	–	–	144.09	126.07
7a	–	61.37	133.04	127.15	–	–
7b	–	62.34	132.69	127.14	–	–
7c	–	62.22	132.23	127.47	144.26	125.58
7d	–	61.68	131.92	127.78	–	–
7e	–	61.76	131.90	127.80	–	–
7f	–	62.31	131.36	127.97	–	–
7g	–	62.31	130.68	128.40	–	–
7h	7.09	61.40	–	–	145.08	125.23
7i	7.10	61.51	–	–	144.74	125.45
7j	7.12	61.84	–	–	144.58	125.49
7k	7.12	61.93	–	–	143.64	125.87
7l	7.15	62.64	–	–	142.60	126.41

 © 2012 Wiley-VCH Verlag GmbH & Co. KGaA, Weinheim

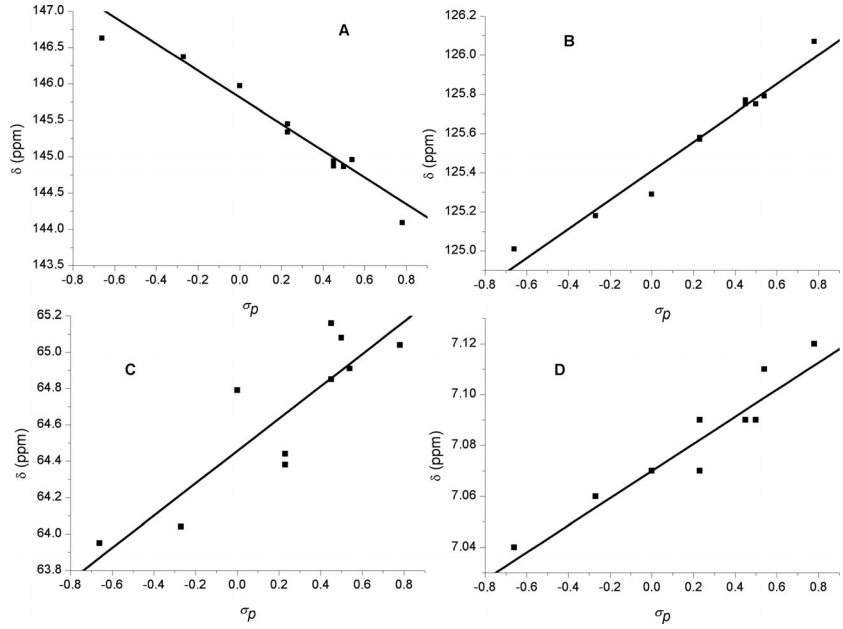

Figure 15. Correlation between NMR chemical shifts (graph A, C-12; graph B, C-15; graph C, C-7; graph D, H-15) and σ_p values in monosubstituted DPNs **5a**–**j**.

tion of the chemical shifts of C-7, C-12, C-15 and H-15 with the σ_p value of the respective group X in monosubstituted DPNs **5a**–**j** are shown. Similar graphs are obtained for FDPNs (see Supporting Information). Although the variations caused by the substituents are, in some cases, not quite significant (e.g. the variations in the chemical shifts in H-15), from the large number of compounds studied some clear trends can be envisaged. First of all, the most sensitive atom to the influence of groups X is the *ipso* carbon atom placed on the adjacent homoconjugated ring (C-12, correlation coefficient of –0.951). The chemical shifts increments in C-12 are higher and show a better linear correlation than that observed for the C-7 carbon atom of the norbornane structure (r^2 = 0.874). This fact confirms that the effects are transmitted through homoconjugative interactions between the aryl rings and not through bonds via C-7. This phenomenon is similar to the transannular π-electronic effect described in cyclophanes.[34–36] The effect of substitution is less pronounced in C-15 and H-15, although there is a good correlation with σ_p in both cases (r^2 = 0.983 and 0.941, respectively).

Conclusions

We have synthesized a large family of aromatic homoconjugated compounds with substituents at the *para* and *meta* positions of the aryl rings, in order to carry out the first systematic study of the interactions between the aromatic moieties in this type of chromophores. The homoconjugative interactions in these compounds are clearly demonstrated by the absorption and NMR spectra, as well as by their reactivity. The UV/Vis spectra show new homoconjugative bands whose wavelength maxima strongly depends on the electronic nature of the substituents (measured by their corresponding σ_p value). TD-DFT calculations assign this homoconjugative bands to transitions involving molecular orbitals which are delocalized on both aryl moieties. On the other hand, the position of the bands of the chromophores placed in one of the aryl rings is influenced by the substituents attached at the *para* position of the cofacially arranged (homoconjugated) aromatic ring. These results are a clear indication of the importance of transannular homoconjugative interactions in the compounds studied in this work. Moreover, push-pull systems show intense intramolecular CT bands which are favoured when the substituents are placed at the *para* positions of the aromatic rings. Substitution at the *meta* position diminishes the homoconjugative interaction. Finally, NMR spectra show that the transannular interactions are transmitted by homoconjugation between the aromatic rings and not through the C-7 carbon atom of the norbornane framework.

In summary, our joint experimental–computational study shows that homoconjugative interactions constitute indeed an effective way to provoke electronic communication which can be easily tuned by controlling the nature and position of the substituents. Thus, the proper selection of the substituents may lead to new organic materials with remarkable optical properties.

Experimental Section

See the Supporting Information for experimental details.

Compound 5a: Yield: 95%. ^{1}H NMR (300 MHz, $CDCl_3$): δ = 7.38 (d, J = 9.0 Hz, 2 H), 7.26–7.15 (m, 4 H), 7.04 (t, J = 9.0 Hz, 1 H), 6.57 (d, J = 9.0 Hz, 2 H), 3.23 (br. s, 2 H), 3.05–2.95 (m, 2 H), 1.80–1.65 (m, 4 H), 1.40–1.20 (m, 4 H) ppm. ^{13}C NMR ($CDCl_3$, 75 MHz): δ = 146.6, 143.5, 136.4, 128.2, 128.0, 127.0, 125.0, 115.2, 64.0, 41.7, 28.5, 28.4 ppm. MS (EI, 70 eV): *m*/*z* (%) = 263 (100)

 © 2012 Wiley-VCH Verlag GmbH & Co. KGaA, Weinheim

[M+], 186 (24), 182 (37), 130 (15), 115 (25), 106 (25), 91 (19). $C_{19}H_{21}N$ (263.38): calcd. C 86.64, H 8.04, N 5.32; found C 86.48, H 8.22, N 5.28.

Compound 5b: Yield: 88%. ^{1}H NMR (300 MHz, $CDCl_3$): δ = 7.39 (d, J = 7.2 Hz, 2 H), 7.32 (d, J = 8.7 Hz, 2 H), 7.20 (t, J = 7.2 Hz, 2 H), 7.06 (t, J = 7.2 Hz, 1 H), 6.75 (d, J = 9.0 Hz, 2 H), 3.71 (s, 3 H), 3.10–3.95 (m, 2 H), 1.70–1.60 (m, 4 H), 1.35–1.25 (m, 4 H) ppm. ^{13}C NMR ($CDCl_3$, 75 MHz): δ = 157.1, 146.4, 138.3, 128.2, 127.1, 125.2, 113.7, 64.0, 55.1, 41.8, 28.5, 28.4 ppm. MS (EI, 70 eV): *m/z* (%) = 278 (100) [M+], 277 (23), 209 (22), 197 (45), 121 (24), 115 (29), 91 (34). $C_{20}H_{22}O$ (278.39): calcd. C 86.28, H 7.97; found C 86.05, H 7.81.

Compound 5d: Yield: 60%. ^{1}H NMR (300 MHz, $CDCl_3$): δ = 7.50–7.30 (m, 4 H), 7.28–7.15 (m, 4 H), 7.09 (t, J = 7.6 Hz, 1 H), 3.10–3.00 (m, 2 H), 1.80–1.50 (m, 4 H), 1.50–1.20 (m, 4 H) ppm. ^{13}C NMR ($CDCl_3$, 75 MHz): δ = 145.4, 144.6, 130.9, 128.7, 128.4, 128.3, 127.1, 125.6, 64.4, 41.7, 28.4, 28.3 ppm. MS (EI, 70 eV): *m/z* (%) = 284 (140) [M+ + 2], 282 (100) [M+], 247 (100), 205 (55), 203 (30), 201 (40), 189 (59), 179 (30), 165 (43), 125 (46), 115 (40), 109 (65), 91 (45), 67 (36), 55 (28). $C_{19}H_{19}Cl$ (282.81): calcd. C 80.68, H 6.78; found C 80.93, H 6.87.

Compound 5e: Yield: 25%. ^{1}H NMR (300 MHz, $CDCl_3$): δ = 7.38 (d, J = 7.3 Hz, 2 H), 7.35–7.25 (m, 4 H), 7.21 (t, J = 7.8 Hz, 2 H), 7.07 (t, J = 7.3 Hz, 1 H), 3.10–2.95 (m, 2 H), 1.72–1.52 (m, 4 H), 1.45–1.25 (m, 4 H) ppm. ^{13}C NMR ($CDCl_3$, 75 MHz): δ = 145.3, 145.1, 131.4, 129.1, 128.4, 127.1, 125.6, 119.1, 64.4, 41.7, 28.4, 28.3 ppm. MS (EI, 70 eV): *m/z* (%) = 328 (31) [M+ + 2], 326 (31) [M+], 247 (71), 205 (35), 204 (27), 193 (31), 192 (80), 191 (55), 189 (25), 179 (35), 178 (35), 169 (37), 166 (27), 165 (58), 143 (30), 141 (26), 129 (45), 128 (28), 117 (40), 115 (49), 101 (29), 95 (28), 91 (100), 77 (22), 51 (19), 41 (29). $C_{19}H_{19}Br$ (327.26): calcd. C 69.71, H 5.85; found C 69.66, H 5.79.

Compound 5f: Yield: 80%. ^{1}H NMR (300 MHz, $CDCl_3$): δ = 7.95 (d, J = 8.4 Hz, 2 H), 7.53 (d, J = 8.7 Hz, 2 H), 7.42 (d, J = 7.2 Hz, 2 H), 7.23 (t, J = 7.2 Hz, 2 H), 7.09 (t, J = 7.5 Hz, 1 H), 3.16–3.06 (m, 2 H), 1.72–1.52 (m, 4 H), 1.40–1.20 (m, 4 H) ppm. ^{13}C NMR ($CDCl_3$, 75 MHz): δ = 172.0, 152.4, 144.9, 130.4, 128.5, 127.4, 127.3, 126.2, 125.8, 65.2, 41.7, 28.2 ppm. MS (EI, 70 eV): *m/z* (%) = 292 (64) [M+], 248 (22), 247 (100), 211 (28), 205 (39), 193 (21), 191 (26), 179 (42), 178 (35), 165 (48), 143 (20), 129 (42), 128 (28), 117 (27), 115 (89), 91 (96), 81 (23), 77 (30), 44 (41), 41 (38). $C_{20}H_{20}O_2$ (292.38): calcd. C 82.15, H 6.90; found C 82.28, H 6.85.

Compound 5g: Yield: 72%. ^{1}H NMR (300 MHz, $CDCl_3$): δ = 7.89 (d, J = 8.7 Hz, 2 H), 7.51 (d, J = 8.7 Hz, 2 H), 7.42 (d, J = 8.7 Hz, 2 H), 7.23 (t, J = 8.7 Hz, 2 H), 7.09 (t, J = 8.7 Hz, 1 H), 4.33 (q, J = 7.2 Hz, 2 H), 3.15–3.05 (m, 2 H), 1.72–1.52 (m, 4 H), 1.40–1.20 (m, 7 H) ppm. ^{13}C NMR ($CDCl_3$, 75 MHz): δ = 167.2, 152.0, 144.9, 129.7, 128.4, 127.4, 127.3, 127.3, 125.7, 64.9, 60.8, 41.6, 28.3, 14.3 ppm. MS (EI, 70 eV): *m/z* (%) = 320 (30) [M+], 248 (21), 247 (100), 205 (32), 191 (28), 179 (20), 178 (24), 165 (36), 143 (22), 129 (33), 117 (35), 115 (51), 91 (77), 77 (15), 41 (19). $C_{22}H_{24}O_2$ (320.43): calcd. C 82.45, H 7.55; found C 82.42, H 7.67.

Compound 5h: Yield: 80%. ^{1}H NMR (300 MHz, $CDCl_3$): δ = 7.81 (d, J = 8.0 Hz, 2 H), 7.51 (d, J = 8.0 Hz, 2 H), 7.41 (d, J = 8.0 Hz, 2 H), 7.21 (t, J = 7.3 Hz, 2 H), 7.09 (t, J = 7.8 Hz, 1 H), 3.15–3.05 (m, 2 H), 2.51 (s, 3 H), 1.72–1.52 (m, 4 H), 1.45–1.20 (m, 4 H) ppm. ^{13}C NMR ($CDCl_3$, 75 MHz): δ = 197.8, 151.8, 144.9, 134.5, 128.6, 128.5, 127.5, 127.3, 125.8, 65.1, 41.6, 28.3, 26.5 ppm. MS (EI, 70 eV): *m/z* (%) = 290 (14) [M+], 91 (11), 43 (100). $C_{21}H_{22}O$ (290.40): calcd. C 86.85, H 7.64; found C 87.04, H 7.57.

Compound 5i: Yield: 82%. ^{1}H NMR (300 MHz, $CDCl_3$): δ = 7.53 (d, J = 9.0 Hz, 2 H), 7.45 (d, J = 9.0 Hz, 2 H), 7.40 (d, J = 8.4 Hz, 2 H), 7.22 (t, J = 7.0 Hz, 2 H), 7.11 (t, J = 7.5 Hz, 1 H), 3.12–3.00 (m, 2 H), 1.70–1.50 (m, 4 H), 1.42–1.28 (m, 4 H) ppm. ^{13}C NMR ($CDCl_3$, 75 MHz): δ = 150.1 (q, J = 1.4 Hz), 145.0, 128.5, 127.6, 127.5 (q, J = 47.0 Hz), 127.3, 125.8, 125.3 (q, J = 3.9 Hz), 124.0 (q, J = 272.0 Hz), 64.9, 41.7, 28.3, 28.2 ppm. MS (EI, 70 eV): *m/z* (%) = 316 (100) [M+], 274 (21), 273 (22), 271 (18), 248 (31), 247 (51), 235 (20), 183 (17), 179 (16), 165 (16), 115 (28), 91 (34), 81 (15). $C_{20}H_{19}F_3$ (316.36): calcd. C 75.91, H 6.06; found C 76.08, H 6.15.

Compound 5j: Yield: 87%. ^{1}H NMR (300 MHz, $CDCl_3$): δ = 8.08 (d, J = 9.0 Hz, 2 H), 7.58 (d, J = 9.0 Hz, 2 H), 7.40 (d, J = 7.8 Hz, 2 H), 7.24 (t, J = 7.8 Hz, 2 H), 7.12 (t, J = 7.8 Hz, 1 H), 3.15–3.05 (m, 2 H), 1.72–1.62 (m, 2 H), 1.60–1.50 (m, 2 H), 1.45–1.30 (m, 4 H) ppm. ^{13}C NMR ($CDCl_3$, 75 MHz): δ = 153.8, 145.8, 144.1, 128.6, 128.0, 127.3, 126.1, 123.8, 65.0, 41.8, 28.2, 28.1 ppm. MS (EI, 70 eV): *m/z* (%) = 293 (94) [M+], 277 (22), 276 (41), 264 (29), 263 (100), 262 (37), 251 (33), 225 (41), 208 (25), 204 (35), 203 (30), 202 (34), 192 (65), 191 (63), 190 (29), 189 (38), 186 (29), 182 (40), 179 (27), 178 (54), 166 (30), 165 (71), 152 (28), 141 (27), 129 (39), 128 (43), 115 (89), 107 (27), 106 (30), 91 (98), 81 (38), 77 (39), 51 (30). $C_{19}H_{19}NO_2$ (293.36): calcd. C 77.78, H 6.53, N 4.78; found C 77.81, H 6.66, N 4.69.

Compound 6a: Yield: 25%. ^{1}H NMR (300 MHz, $CDCl_3$): δ = 7.24 (d, J = 9.9 Hz, 4 H), 6.60 (d, J = 9.9 Hz, 4 H), 3.00–2.90 (m, 2 H), 2.84 (s, 12 H), 1.70–1.60 (m, 4 H), 1.32–1.22 (m, 4 H) ppm. ^{13}C NMR ($CDCl_3$, 75 MHz): δ = 148.0, 135.3, 127.6, 112.7, 62.8, 41.7, 40.7, 28.7 ppm. MS (EI, 70 eV): *m/z* (%) = 334 (100) [M+], 333 (49), 290 (33), 253 (33), 213 (33), 167 (31), 146 (21), 139 (33), 138 (35), 134 (74), 131 (59), 126 (42), 118 (31), 117 (32), 44 (19), 42 (26). $C_{23}H_{30}N_2$ (334.50): calcd. C 82.58, H 9.05, N 8.38; found C 82.71, H 9.20, N 8.27.

Compound 6b: Yield: 97%. ^{1}H NMR (300 MHz, $CDCl_3$): δ = 7.16 (d, J = 8.7 Hz, 4 H), 6.54 (d, J = 8.4 Hz, 4 H), 3.39 (br. s, 4 H), 2.98–2.90 (m, 2 H), 1.72–1.58 (m, 4 H), 1.80–1.40 (m, 4 H) ppm. ^{13}C NMR ($CDCl_3$, 75 MHz): δ = 143.3, 137.1, 127.8, 115.2, 63.1, 41.7, 28.5 ppm. MS (EI, 70 eV): *m/z* (%) = 278 (100) [M+], 277 (42), 197 (36), 185 (27), 144 (20), 130 (32), 106 (64), 91 (6), 77 (13). $C_{19}H_{22}N_2$ (278.40): calcd. C 81.96, H 7.97, N 10.07; found C 82.12, H 7.73, N 10.18.

Compound 6c: Yield: 85%. ^{1}H NMR (300 MHz, $CDCl_3$): δ = 7.29 (d, J = 6.7 Hz, 4 H), 6.74 (d, J = 6.7 Hz, 4 H), 3.70 (s, 6 H), 3.02–2.95 (m, 2 H), 1.70–1.55 (m, 4 H), 1.35–1.20 (m,4 H) ppm. ^{13}C NMR ($CDCl_3$, 75 MHz): δ = 157.0, 138.7, 128.0, 113.6, 63.3, 55.4, 41.9, 28.5 ppm. MS (EI, 70 eV): *m/z* (%) = 308 (80) [M+], 277 (55), 227 (50), 200 (23), 159 (23), 145 (30), 121 (100), 91 (25). $C_{21}H_{24}O_2$ (308.42): calcd. C 81.77, H 7.85; found C 81.88, H 7.97.

Compound 6e: Yield: 90%. ^{1}H NMR (300 MHz, [D$_6$]DMSO): δ = 12.80 (br. s, 2 H), 7.79 (d, J = 8.7 Hz, 4 H), 7.64 (d, J = 8.7 Hz, 4 H), 3.30–3.24 (m, 2 H), 1.58–1.40 (m, 4 H), 1.40–1.20 (m, 4 H) ppm. ^{13}C NMR (75 MHz, [D$_6$]DMSO): δ = 172.1, 151.8, 130.8, 129.5, 128.8, 66.5, 42.7, 29.0 ppm. MS (EI, 70 eV): *m/z* (%) = 336 (17) [M+], 292 (26), 291 (100), 205 (25), 191 (19), 189 (18), 179 (24), 178 (26), 165 (29), 143 (20), 135 (25), 129 (36), 128 (20), 117 (26), 115 (60), 91 (51), 81 (46), 77 (24), 44 (72), 41 (31). $C_{21}H_{20}O_4$ (336.39): calcd. C 74.97, H 6.00; found C 74.82, H 6.13.

Compound 6f: Yield: 72%. ^{1}H NMR (300 MHz, $CDCl_3$): δ = 7.90 (d, J = 8.7 Hz, 4 H), 7.48 (d, J = 8.7 Hz, 4 H), 4.33 (q, J = 7.2 Hz, 4 H), 3.15–3.05 (m, 2 H), 1.70–1.55 (m, 4 H), 1.42–1.26 (m, 10 H) ppm. ^{13}C NMR ($CDCl_3$, 75 MHz): δ = 166.4, 150.3, 129.8, 128.0, 127.3, 65.3, 60.7, 41.7, 28.2, 14.3 ppm. MS (EI, 70 eV): *m/z* (%) = 392 (11) [M+], 347 (18), 320 (24), 319 (100), 205 (17), 191 (19), 165

 © 2012 Wiley-VCH Verlag GmbH & Co. KGaA, Weinheim

(25), 143 (24), 129 (30), 117 (31), 115 (30), 91 (28), 77 (10), 41 (16). $C_{25}H_{28}O_4$ (392.49): calcd. C 76.49, H 7.19; found C 76.57, H 7.25.

Compound 6g: Yield: 85%. ^{1}H NMR (300 MHz, $CDCl_3$): δ = 7.83 (d, J = 8.4 Hz, 4 H), 7.51 (d, J = 8.4 Hz, 4 H), 3.18–3.08 (m, 2 H), 2.51 (s, 6 H), 1.69–1.58 (m, 4 H), 1.45–1.30 (m, 4 H) ppm. ^{13}C NMR ($CDCl_3$, 75 MHz): δ = 197.6, 150.5, 134.8, 128.7, 127.6, 65.3, 41.7, 28.2, 26.5 ppm. MS (EI, 70 eV): *m*/*z* (%) = 332 (10) [M$^+$], 289 (8), 151 (8), 43 (100). $C_{23}H_{24}O_2$ (332.44): calcd. C 83.09, H 7.28; found C 82.92, H 7.33.

Compound 6h: Yield: 94%. ^{1}H NMR (300 MHz, $CDCl_3$): δ = 8.12 (d, J = 9.0 Hz, 4 H), 7.58 (d, J = 9.0 Hz, 4 H), 3.18–3.10 (m, 2 H), 1.65–1.55 (m, 4 H), 1.50–1.40 (m, 4 H) ppm. ^{13}C NMR ($CDCl_3$, 75 MHz): δ = 151.7, 146.0, 128.1, 124.0, 65.4, 41.9, 28.0 ppm. MS (EI, 70 eV): *m*/*z* (%) = 338 (14) [M$^+$], 308 (37), 279 (36), 278 (100), 277 (41), 197 (37), 189 (24), 186 (30), 185 (28), 149 (28), 144 (24), 130 (33), 106 (69). $C_{19}H_{18}N_2O_4$ (338.36): calcd. C 67.43, H 5.36, N 8.28; found C 67.48, H 5.44, N 8.32.

Compound 7d: Yield: 63%. ^{1}H NMR (300 MHz, $CDCl_3$): δ = 7.50–7.35 (m, 3 H), 7.20 (d, J = 8.5 Hz, 2 H), 7.13–6.97 (m, 2 H), 6.88 (ddd, J = 12.0, 8.0, 1.4 Hz, 1 H), 3.35 (dt, J = 4.3, 4.3 Hz), 3.10–2.95 (m, 1 H), 1.84–1.65 (m, 2 H), 1.55–1.20 (m, 6 H) ppm. ^{13}C NMR ($CDCl_3$, 75 MHz): δ = 161.7 (d, J = 246.7 Hz), 142.8, 131.9 (d, J = 13.6 Hz), 131.3, 129.4 (d, J = 5.6 Hz), 129.1, 129.1, 128.3, 127.8 (d, J = 8.8 Hz), 124.1 (d, J = 3.2 Hz), 116.3 (d, J = 23.9 Hz), 61.7 (d, J = 2.5 Hz), 42.5, 41.3 (d, J = 8.1 Hz), 28.9, 28.3, 28.1, 27.2 ppm. MS (EI, 70 eV): *m*/*z* (%) = 302 (14) [M$^+$ + 2], 300 (46) [M$^+$], 282 (35), 265 (51), 247 (36), 232 (47), 223 (49), 221 (28), 219 (52), 210 (30), 209 (27), 203 (27), 201 (28), 197 (25), 191 (25), 183 (44), 165 (36), 149 (38), 143 (28), 133 (33), 129 (41), 127 (34), 125 (59), 117 (37), 115 (57), 108 (100), 101 (37), 91 (52), 81 (35), 41 (35). $C_{19}H_{18}ClF$ (300.80): calcd. C 75.85, H 6.03; found C 75.69, H 6.12.

Compound 7e: Yield: 62%. ^{1}H NMR (300 MHz, $CDCl_3$): δ = 7.46 (td, J = 7.4 Hz, 1 H), 7.35 (s, 4 H), 7.15–7.00 (m, 2 H), 6.88 (ddd, J = 12.1, 8.1, 1.5 Hz, 1 H), 3.41–3.32 (m, 1 H), 3.08–3.00 (m, 1 H), 1.84–1.65 (m, 2 H), 1.55–1.20 (m, 6 H) ppm. ^{13}C NMR ($CDCl_3$, 75 MHz): δ = 161.7 (d, J = 246.7 Hz), 143.3, 131.9 (d, J = 13.6 Hz), 131.2, 129.5, 129.5, 129.4 (d, J = 5.6 Hz), 127.8 (d, J = 8.7 Hz), 124.1 (d, J = 3.2 Hz), 119.4, 116.3 (d, J = 23.9 Hz), 61.8 (d, J = 2.5 Hz), 42.5, 41.3 (d, J = 8.1 Hz), 28.9, 28.3, 28.1, 27.2 ppm. MS (EI, 70 eV): *m*/*z* (%) = 346 (33) [M$^+$ + 2], 344 (35) [M$^+$], 278 (30), 276 (30), 265 (65), 263 (39), 223 (58), 210 (87), 196 (37), 183 (60), 169 (38), 161 (16), 143 (41), 135 (46), 115 (43), 109 (100), 91 (30), 81 (48), 67 (25), 41 (50). $C_{19}H_{18}BrF$ (345.25): calcd. C 66.08, H 5.26; found C 66.14, H 5.16.

Compound 7f: Yield: 75%. ^{1}H NMR (300 MHz, $CDCl_3$): δ = 7.83 (d, J = 8.5 Hz, 2 H), 7.57 (d, J = 8.2 Hz, 2 H), 7.49 (td, J = 7.6, 2.0 Hz, 1 H), 7.15–6.95 (m, 2 H), 6.88 (ddd, J = 12.0, 7.9, 1.4 Hz, 1 H), 3.40 (dt, J = 4.3, 4.3 Hz, 1 H), 3.12–3.05 (m, 1 H), 2.50 (s, 3 H), 1.82–1.20 (m, 8 H) ppm. ^{13}C NMR ($CDCl_3$, 75 MHz): δ = 197.8, 160.8 (d, J = 246.9 Hz), 149.9, 134.7, 131.4 (d, J = 13.5 Hz), 129.5 (d, J = 5.4 Hz), 128.4, 128.0 (d, J = 8.7 Hz), 127.9, 128.0, 124.2 (d, J = 3.2 Hz), 116.3 (d, J = 23.9 Hz), 62.3 (d, J = 2.6 Hz), 42.5, 41.2 (d, J = 8.2 Hz), 28.8, 28.3, 28.1, 27.2, 26.5 ppm. MS (EI, 70 eV): *m*/*z* (%) = 308(14) [M$^+$], 225 (9), 43 (100). $C_{21}H_{21}FO$ (308.39): calcd. C 81.78, H 6.87; found C 81.94, H 6.68.

Compound 7k: Yield 87%. ^{1}H NMR (300 MHz, $CDCl_3$): δ = 7.44 (d, J = 8.1 Hz, 2 H), 7.37 (t, J = 8.46 Hz, 1 H), 7.12 (t, J = 8.09 Hz, 2 H), 7.20–7.04 (m, 3 H), 3.39 (dt, J = 4.1, 4.1 Hz, 1 H), 3.08–3.00 (m, 1 H), 1.82–1.65 (m, 2 H), 1.60–1.20 (m, 6 H) ppm. ^{13}C NMR ($CDCl_3$, 75 MHz): δ = 160.6 (d, J = 251.5 Hz), 143.6, 131.9 (d, J = 13.6 Hz), 130.8 (d, J = 6.8 Hz), 128.3, 127.5, 127.5, 127.3 (d, J = 3.2 Hz), 125.9, 119.8 (d, J = 27.9 Hz), 119.5 (d, J = 10.0 Hz), 61.9 (d, J = 3.1 Hz), 42.5, 41.1 (d, J = 8.4 Hz), 28.8, 28.4, 28.0, 27.2 ppm. MS (EI, 70 eV): *m*/*z* (%) = 346 (29) [M$^+$ + 2], 344 (37) [M$^+$], 278 (23), 276 (24), 265 (59), 263 (34), 223 (23), 222 (27), 211 (30), 210 (84), 209 (62), 207 (20), 197 (47), 196 (41), 189 (58), 187 (57), 183 (57), 170 (19), 157 (21), 144 (21), 133 (24), 129 (33), 116 (36), 115 (48), 107 (24), 104 (34), 94 (28), 91 (100), 81 (42), 79 (26), 77 (24), 65 (23), 51 (27), 41 (43). $C_{19}H_{18}BrF$ (345.25): calcd. C 66.08, H 5.26; found C 65.89, H 5.15.

Compound 7v: Yield: 74%. ^{1}H NMR (300 MHz, $CDCl_3$): δ = 8.08 (d, J = 9.0 Hz, 2 H), 7.58 (dd, J = 9.0, 1.5 Hz, 2 H), 7.19 (t, J = 8.6 Hz, 1 H), 6.37 (dd, J = 8.6, 2.4 Hz, 1 H), 6.22 (dd, J = 13.5, 2.4 Hz, 1 H), 3.64 (br. s, 2 H), 3.34 (dt, J = 3.6, 3.6 Hz, 1 H), 3.07–2.95 (m, 1 H), 1.93–1.07 (m, 8 H) ppm. ^{13}C NMR ($CDCl_3$, 75 MHz): δ = 161.5 (d, J = 245.4 Hz), 152.9, 146.8 (d, J = 11.5 Hz), 145.7, 130.0 (d, J = 7.45 Hz), 128.3, 128.2, 123.5, 120.4 (d, J = 14.4 Hz), 111.1 (d, J = 2.3 Hz), 102.8 (d, J = 27.3 Hz), 61.6 (d, J = 2.7 Hz), 42.6, 41.4 (d, J = 8.2 Hz), 28.8, 28.3, 28.1, 27.2 ppm. MS (EI, 70 eV): *m*/*z* (%) = 326 (100) [M$^+$], 309 (28), 271 (17), 258 (18), 225 (22), 224 (19), 124 (25), 111 (17), 57 (17). $C_{19}H_{19}FN_2O_2$ (326.37): calcd. C 69.91, H 5.87, N 8.59; found C 69.83, H 5.97, N 8.63.

Compound 8: Yield: 60%. ^{1}H NMR (300 MHz, $CDCl_3$): δ = 8.42 (dd, J = 6.6, 2.9 Hz, 1 H), 8.14 (d, J = 9.1 Hz, 2 H), 8.07 (ddd, J = 9.0, 4.2, 2.9 Hz, 1 H), 7.65 (dd, J = 9.1, 1.5 Hz, 2 H), 7.08 (dd, J = 9.1, 9.0 Hz, 1 H), 3.51–3.38 (m, 1 H), 3.29–3.17 (m, 1 H), 1.90–1.62 (m, 2 H), 1.60–1.31 (m, 6 H) ppm. ^{13}C NMR ($CDCl_3$, 75 MHz): δ = 164.4 (d, J = 258.5 Hz), 150.1, 146.4, 143.0 (d, J = 2.9 Hz), 132.8 (d, J = 16.0 Hz), 128.7, 128.7, 125.6 (d, J = 7.5 Hz), 124.4 (d, J = 10.8 Hz), 123.9, 117.5 (d, J = 29.5 Hz), 62.4 (d, J = 2.7 Hz), 43.0, 41.3 (d, J = 7.5 Hz), 28.6, 28.1, 27.8, 27.0 ppm. MS (EI, 70 eV): *m*/*z* (%) = 356 (100) [M$^+$], 339 (59), 297 (46), 267 (34), 207 (34), 81 (54), 67 (36). $C_{19}H_{17}FN_2O_4$ (356.35): calcd. C 64.02, H 4.81, N 7.86; found C 64.21, H 4.69, N 7.73.

Compound 10b: Yield: 95%. ^{1}H NMR (300 MHz, $CDCl_3$): δ = 7.24 (d, J = 6.6, Hz, 2 H), 6.75 (d, J = 6.6, Hz, 2 H), 6.60 (d, J = 2.3 Hz, 1 H), 6.47 (d, J = 8.0 Hz, 1 H), 6.40 (dd, J = 8.0, 2.3 Hz, 1 H), 3.82–3.13 (m, 4 H), 3.06–2.89 (m, 1 H), 2.07–1.77 (m, 6 H), 1.77–1.43 (m, 2 H) ppm. ^{13}C NMR ($CDCl_3$, 75 MHz): δ = 145.3, 144.5, 144.4, 137.2, 135.3, 128.6, 124.4, 115.0, 112.1, 111.1, 41.4, 35.2, 32.6, 27.3 ppm. MS (EI, 70 eV): *m*/*z* (%) = 264 (99) [M$^+$], 263 (13), 236 (90), 235 (100), 221 (37), 218 (20), 149 (26), 106 (19), 69 (29), 57 (8). $C_{18}H_{20}N_2$ (264.37): calcd. C 81.77, H 7.63, N 10.60; found C 81.60, H 7.79, N 10.58.

Compound 10c: Yield: 25%. ^{1}H NMR (300 MHz, $CDCl_3$): δ = 8.33 (d, J = 7.0 Hz, 2 H), 8.11 (d, J = 2.4 Hz, 1 H), 7.96 (dd, J = 8.4, 2.4 Hz, 1 H), 7.61 (d, J = 7.0 Hz, 2 H), 6.71 (d, J = 8.4 Hz, 1 H), 3.35–3.29 (m, 1 H), 2.14–2.0 (m, 4 H), 2.0–1.88 (m, 2 H), 1.73–1.59 (m, 2 H) ppm. ^{13}C NMR ($CDCl_3$, 75 MHz): δ = 152.1, 151.1, 147.0, 146.7, 145.4, 128.8, 124.0, 123.8, 121.4, 119.1, 44.1, 35.1, 31.8, 26.4 ppm. MS (EI, 70 eV): *m*/*z* (%) = 324 (100) [M$^+$], 296 (56), 295 (86), 279 (26), 250 (38), 249 (95), 204 (34), 203 (67), 202 (94), 189 (29), 136 (17), 101 (14), 77 (25). $C_{18}H_{16}N_2O_4$ (324.34): calcd. C 73.94, H 5.52, N 9.59; found C 74.12, H 5.71, N 9.82.

Compound 11: Yield: 31%. ^{1}H NMR (300 MHz, $CDCl_3$): δ = 8.08 (d, J = 9.0 Hz, 2 H), 8.14 (dd, J = 9.0, 1.5 Hz, 2 H), 6.79–6.63 (m, 2 H), 6.42 (ddd, J = 8.5, 3.9, 2.9 Hz, 1 H), 3.43–3.34 (m, 3 H), 3.04–2.96 (m, 1 H), 1.95–1.77 (m, 1 H), 1.70–1.52 (m, 2 H), 1.47–1.35 (m, 5 H) ppm. ^{13}C NMR ($CDCl_3$, 75 MHz): δ = 154.3 (d, J = 237.5 Hz), 152.1, 145.9, 142.6 (d, J = 2.0 Hz), 131.1 (d, J = 14.7 Hz), 128.6, 128.6, 123.5, 116.9 (d, J = 25.5 Hz), 115.5 (d, J =

 © 2012 Wiley-VCH Verlag GmbH & Co. KGaA, Weinheim

4.9 Hz), 114.8 (d, J = 8.5 Hz), 62.4 (d, J = 2.8 Hz), 42.6, 41.4 (d, J = 8.4 Hz), 28.9, 28.3, 28.2, 27.2 ppm. MS (EI, 70 eV): *m/z* (%) = 326 (100) [M^+], 283 (15), 258 (17), 138 (27), 124 (14), 81 (10). $C_{19}H_{19}FN_2O_2$ (326.37): calcd. C 69.91, H 5.87, N 8.59; found C 69.86, H 5.99, N 8.45.

Compound 12: Yield: 30%. ^{1}H NMR (300 MHz, $CDCl_3$): δ = 8.37 (dd, J = 6.6, 2.9 Hz, 1 H), 7.97 (ddd, J = 9.0, 4.1, 2.9 Hz, 1 H), 7.23 (dd, J = 8.6, 1.5 Hz, 2 H), 7.01 (dd, J = 9.0, 8.5 Hz, 1 H), 6.57 (d, J = 8.6 Hz, 2 H), 3.65–3.48 (br. s, 2 H), 3.37–3.27 (m, 1 H), 3.09 (t, J = 3.8 Hz, 1 H), 1.86–1.61 (m, 2 H), 1.61–1.18 (m, 6 H) ppm. ^{13}C NMR ($CDCl_3$, 75 MHz): δ = 164.4 (d, J = 258.3 Hz), 144.6, 144.2 (d, J = 2.5 Hz), 135.1 (d, J = 16.1 Hz), 132.8, 128.6, 128.5, 125.5 (d, J = 8.2 Hz), 123.2 (d, J = 10.8 Hz), 117.2 (d, J = 27.0 Hz), 115.1, 61.6 (d, J = 3.0 Hz), 42.8, 41.2 (d, J = 8.2 Hz), 28.8, 28.5, 28.0, 27.2 ppm. MS (EI, 70 eV): *m/z* (%) = 326 (100) [M^+], 271 (20), 245 (35), 225 (15), 106 (12), 93 (11). $C_{19}H_{19}FN_2O_2$ (326.37): calcd. C 69.91, H 5.87, N 8.59; found C 70.12, H 5.76, N 8.71.

Compound 15: Yield: 65%. ^{1}H NMR (300 MHz, $CDCl_3$): δ = 7.75 (br. s, 1 H), 7.56–7.40 (m, 3 H), 7.35–7.05 (m, 5 H), 3.40 (dt, J = 3.9, 3.9 Hz, 1 H), 3.05 (t, J = 3.2 Hz, 1 H), 1.85–1.61 (m, 2 H), 1.61–1.20 (m, 6 H) ppm. ^{13}C NMR ($CDCl_3$, 75 MHz): δ = 160.6 (d, J = 248.1 Hz), 154.6 (d, J = 37.6 Hz), 143.8, 134.1 (d, J = 11.2 Hz), 130.9 (d, J = 14.1 Hz), 130.3 (d, J = 7.0 Hz), 128.3, 128.3, 127.6, 127.5, 125.9, 115.8 (d, J = 3.2 Hz), 115.6 (q, J = 288.8 Hz), 108.9 (d, J = 29.7 Hz), 62.0 (d, J = 2.9 Hz), 42.6, 41.2 (d, J = 8.0 Hz), 28.9, 28.5, 28.1, 27.3 ppm. MS (EI, 70 eV): *m/z* (%) = 378, (24) [M^+ + H] 377 (100) [M^+], 335 (26), 309 (36), 308 (19), 296 (40), 220 (27), 115 (17), 91 (29), 84 (28), 51 (22), 49 (55). $C_{21}H_{19}F_4NO$ (377.38): calcd. C 66.82, H 5.08, N 3.71; found C 66.89, H 5.19, N 3.64.

Compound 16: Yield: 77%. ^{1}H NMR (300 MHz, $CDCl_3$): δ = 8.10 (d, J = 9.0 Hz, 2 H), 7.98 (br. s, 1 H), 7.61 (dd, J = 9.0, 1.5 Hz, 2 H), 7.55–7.43 (m, 1 H), 7.36 (dd, J = 12.9, 2.2 Hz, 1 H), 7.20 (dd, J = 8.4, 2.2 Hz, 1 H), 3.47–3.34 (m, 1 H), 3.14–3.02 (m, 1 H), 1.90–1.15 (m, 8 H) ppm. ^{13}C NMR ($CDCl_3$, 75 MHz): δ = 160.7 (d, J = 248.3 Hz), 154.7 (d, J = 37.6 Hz), 151.5, 146.1, 135.1 (d, J = 11.5 Hz), 130.1 (d, J = 6.6 Hz), 129.0 (d, J = 14.1 Hz), 128.5, 128.5, 123.7, 116.2 (d, J = 3.2 Hz), 115.5 (q, J = 288.8 Hz), 109.1 (d, J = 29.6 Hz), 62.2 (d, J = 2.8 Hz), 42.7, 41.3 (d, J = 7.6 Hz), 28.8, 28.2, 28.0, 27.1 ppm. MS (EI, 70 eV): *m/z* (%) = 423 (24) [M^+ + H], 422 (100) [M^+], 405 (53), 392 (32), 363 (27), 354 (73), 333 (21), 321 (33), 220 (28), 91 (17), 81 (41), 57 (27), 55 (30). $C_{21}H_{18}F_4N_2O_3$ (422.38): calcd. C 59.70, H 4.30, N 6.63; found C 59.58, H 4.49, N 6.51.

Supporting Information (see footnote on the first page of this article): Experimental procedures, UV/Vis spectra, NMR correlations, molecular orbitals, and Cartesian coordinates of all species discussed in the text.

Acknowledgments

Financial support by the Spanish Ministerio de Ciencia e Innovación (MICINN) [grant numbers CTQ2007-67103-C02-01, CTQ2007-67730-C02-01 and Consolider-Ingenio 2010 (CSD2007-0006)] and the Comunidad Autónoma de Madrid (CAM) (P2009/PPQ1634-AVANCAT) is acknowledged. I. F. is a Ramón y Cajal Fellow.

[1] R. Gompper, H.-U. Wagner, *Angew. Chem.* **1988**, *100*, 1492; *Angew. Chem. Int. Ed. Engl.* **1988**, *27*, 1437–1455.

[2] a) G. Jayamurugan, J.-P. Gisselbrecht, C. Boudon, F. Schoenebeck, W. B. Schweizer, B. Bernet, F. Diederich, *Chem. Commun.* **2011**, *47*, 4520–4522; b) Y.-L. Wu, F. Bureš, P. D. Jarowski, W. B. Schweizer, C. Boudon, J.-P. Gisselbrecht, F. Diederich, *Chem. Eur. J.* **2010**, *16*, 9592–9605; c) F. Bureš, W. B. Schweizer, J. C. May, C. Boudon, J.-P. Gisselbrecht, M. Gross, I. Biaggio, F. Diederich, *Chem. Eur. J.* **2007**, *13*, 5378–5387.

[3] W. Akemann, D. Laage, P. Plaza, M. M. Martin, M. Blanchard-Desce, *J. Phys. Chem. B* **2008**, *112*, 358–368.

[4] a) M. Moreno Oliva, J. Casado, M. M. M. Raposo, A. M. C. Fonseca, H. Hartmann, V. Hernández, J. T. López Navarrete, *J. Org. Chem.* **2006**, *71*, 7509–7520; b) B. Milián, E. Ortí, V. Hernández, J. T. López Navarrete, T. Otsubo, *J. Phys. Chem. B* **2003**, *107*, 12175–12183.

[5] a) *Electronic Materials: The Oligomeric Approach* (Eds.: K. Müllen, G. Wegner), Wiley-VCH, Weinheim, **1998**; b) *Handbook of Conducting Polymers* (Eds.: T. A. Skotheim, J. R. Reynolds), CRC Press, Boca Raton, **2007**.

[6] a) *Chem. Rev.* **2007**, *107*, issue 4, special issue on organic electronics and optoelectronics; b) *J. Mater. Res.* **2004**, *19*, issue 7, special issue on organic electronics; c) G. S. He, L.-S. Tan, Q. Zheng, P. N. Prasad, *Chem. Rev.* **2008**, *108*, 1245–1330; d) J. W. Verhoeven, H. J. Van Ramesdonk, M. M. Groeneveld, A. C. Benniston, A. Harriman, *ChemPhysChem* **2005**, *6*, 2251–2260.

[7] a) S. Barlow, S. R. Marder, in: *Functional Organic Materials* (Eds.: T. J. J. Müller, U. H. F. Bunz), Wiley-VCH, Weinheim, Germany, **2007**, pp. 393–437; b) *Chem. Phys.* **1999**, *245*, special issue on molecular nonlinear optics; c) J. Zyss, P. Kelley, P. F. Liao, *Molecular Nonlinear Optics: Materials, Physics and Devices*, Academic Press, **1993**.

[8] *Molecular Wires. From Design to Properties* (Ed.: L. de Cola), thematic issue, *Top. Curr. Chem.* **2005**, *257*, 1–170.

[9] a) P. Milosevic, S. Hecht, *Org. Lett.* **2005**, *7*, 5023–5026; b) F. Würthner, G. Archetti, R. Schmidt, H.-G. Kuball, *Angew. Chem.* **2008**, *120*, 4605; *Angew. Chem. Int. Ed.* **2008**, *47*, 4529–4532; c) H. Hartmann, K. Eckert, A. Schröder, *Angew. Chem.* **2000**, *112*, 567; *Angew. Chem. Int. Ed.* **2000**, *39*, 556–558.

[10] O. Ostroverkhova, W. E. Moerner, *Chem. Rev.* **2004**, *104*, 3267–3314.

[11] a) S.-I. Kato, F. Diederich, *Chem. Commun.* **2010**, *46*, 1994–2006; b) B. Breiten, I. Biaggio, F. Diederich, *Chimia* **2010**, *64*, 409–413; c) S.-I. Kato, M. Kivala, W. B. Schweizer, C. Boudon, J.-P. Gisselbrecht, F. Diederich, *Chem. Eur. J.* **2009**, *15*, 8687–8691. See also: d) S. Sergeyev, D. Didier, V. Boitsov, A. Teshome, I. Asselberghs, K. Clays, C. M. L. Vande Velde, A. Plaquet, B. Champagne, *Chem. Eur. J.* **2010**, *16*, 8181–8190.

[12] A. Ortiz, B. Insausty, M. R. Torres, M. Á. Herranz, N. Martín, R. Viruela, E. Ortí, *Eur. J. Org. Chem.* **2008**, 99–108.

[13] R. Gómez, C. Seoane, J. L. Segura, *Chem. Soc. Rev.* **2007**, *36*, 1305–1322.

[14] a) A. B. Ricks, G. C. Solomon, M. T. Colvin, A. M. Scott, K. Chen, M. A. Ratner, M. R. Wasielewski, *J. Am. Chem. Soc.* **2010**, *132*, 15427–15434; b) R. P. Ortiz, R. M. Osuna, V. Hernández, J. T. López Navarrete, B. Vercelli, G. Zotti, V. V. Sumerin, E. S. Balenkova, V. G. Nenajdenko, *J. Phys. Chem. A* **2007**, *111*, 841–851; c) C. A. van Walree, V. E. M. Kaats-Richters, S. J. Veen, B. Wieczorek, J. H. van der Wiel, B. C. van der Wiel, *Eur. J. Org. Chem.* **2004**, 3046–3056.

[15] F. Rizzo, M. Cavazzini, S. Righetto, F. De Angelis, S. Fantacci, S. Quici, *Eur. J. Org. Chem.* **2010**, 4004–4016; see also ref. [20].

[16] R. H. Goldsmith, J. Vura-Weis, A. M. Scott, S. Borkar, A. Sen, M. A. Ratner, M. Wasielewski, *J. Am. Chem. Soc.* **2008**, *130*, 7659–7669.

[17] For recent reviews on triptycenes, see: a) L. Zhao, Z. Li, T. Wirth, *Chem. Lett.* **2010**, *39*, 658–667; b) J. H. Chong, M. J. MacLachlan, *Chem. Soc. Rev.* **2009**, *38*, 3301–3315; c) T. M. Swager, *Acc. Chem. Res.* **2008**, *41*, 1181–1189; d) J.-S. Yang, J.-L. Yan, *Chem. Commun.* **2008**, 1501–1512. See also: V. R. Skvarchenko, V. K. Shalaev, E. I. Klabunovskii, *Russ. Chem. Rev.* **1974**, *43*, 951–966.

[18] a) T. Nakazawa, I. Murata, *J. Am. Chem. Soc.* **1977**, *99*, 1996–1997; b) K. Yamamura, T. Nakazawa, I. Murata, *Angew.*

 © 2012 Wiley-VCH Verlag GmbH & Co. KGaA, Weinheim

Chem. **1980**, *92*, 565; *Angew. Chem. Int. Ed. Engl.* **1980**, *19*, 543–546; c) K. Yamamura, K. Nakasuji, H. Yamochi, *Chem. Lett.* **1983**, 627–630.
[19] a) X. Gu, Y.-H. Lai, *Org. Lett.* **2010**, *12*, 5200–5203; b) V. J. Chebny, T. S. Navale, R. Shukla, S. V. Lindeman, R. Rathore, *Org. Lett.* **2009**, *11*, 2253–2256; c) T. Doerner, R. Gleiter, F. A. Neugebauer, *Eur. J. Org. Chem.* **1998**, 1615–1623; d) H.-D. Martin, B. Mayer, *Angew. Chem.* **1983**, *95*, 281; *Angew. Chem. Int. Ed. Engl.* **1983**, *22*, 283–314.
[20] S. Kato, M. T. R. Beels, P. La Porta, W. B. Schweizer, C. Boudon, J.-P. Gisselbrecht, F. Diederich, *Angew. Chem. Int. Ed.* **2010**, *49*, 6207–6211.
[21] A. García Martínez, J. Osío Barcina, A. De Fresno Cerezo, R. Gutiérrez Rivas, *J. Am. Chem. Soc.* **1998**, *120*, 673–679.
[22] A. García Martínez, J. Osío Barcina, A. de Fresno Cerezo, G. Rojo, F. Agulló-López, *J. Phys. Chem. B* **2000**, *104*, 43–47.
[23] J. Osío Barcina, N. Herrero-García, F. Cucinotta, L. De Cola, P. Contreras-Carballada, R. M. Williams, A. Guerrero-Martínez, *Chem. Eur. J.* **2010**, *16*, 6033–6040.
[24] a) A. García Martínez, J. Osío Barcina, A. de Fresno Cerezo, A.-D. Schlüter, J. Frahn, *Adv. Mater.* **1999**, *11*, 27–31; b) J. Osío Barcina, M. R. Colorado Heras, M. Mba, R. Gómez Aspe, N. Herrero García, *J. Org. Chem.* **2009**, *74*, 7148–7156.
[25] N. Caraballo-Martínez, M. R. Colorado Heras, M. M. Blázquez, J. Osío Barcina, A. García Martínez, M. R. Torres Salvador, *Org. Lett.* **2007**, *9*, 2943–2946.
[26] N. Herrero-García, I. Fernández, J. Osío Barcina, *Chem. Eur. J.* **2011**, *17*, 7327–7335.
[27] M. J. Frisch, G. W. Trucks, H. B. Schlegel, G. E. Scuseria, M. A. Robb, J. R. Cheeseman, G. Scalmani, V. Barone, B. Mennucci, G. A. Petersson, H. Nakatsuji, M. Caricato, X. Li, H. P. Hratchian, A. F. Izmaylov, J. Bloino, G. Zheng, J. L. Sonnenberg, M. Hada, M. Ehara, K. Toyota, R. Fukuda, J. Hasegawa, M. Ishida, T. Nakajima, Y. Honda, O. Kitao, H. Nakai, T. Vreven, J. A. Montgomery Jr, J. E. Peralta, F. Ogliaro, M. Bearpark, J. J. Heyd, E. Brothers, K. N. Kudin, V. N. Staroverov, R. Kobayashi, J. Normand, K. Raghavachari, A. Rendell, J. C. Burant, S. S. Iyengar, J. Tomasi, M. Cossi, N. Rega, J. M. Millam, M. Klene, J. E. Knox, J. B. Cross, V. Bakken, C. Adamo, J. Jaramillo, R. Gomperts, R. E. Stratmann, O. Yazyev, A. J. Austin, R. Cammi, C. Pomelli, J. W. Ochterski, R. L. Martin, K. Morokuma, V. G. Zakrzewski, G. A. Voth, P. Salvador, J. J. Dannenberg, S. Dapprich, A. D. Daniels, Ö. Farkas, J. B. Foresman, J. V. Ortiz, J. Cioslowski, D. J. Fox, *Gaussian 09*, rev. B.01, Gaussian, Inc., Wallingford CT, **2009**.
[28] Y. Zhao, D. G. Truhlar, *Acc. Chem. Res.* **2008**, *41*, 157–167.
[29] W. J. Hehre, L. Radom, P. v. R. Schleyer, J. A. Pople, *Ab initio Molecular Orbital Theory*, Wiley, New York, **1986**, p. 76, and references cited therein.
[30] a) M. E. Casida, *Recent Developments and Applications of Modern Density Functional Theory*, vol. 4, Elsevier, Amsterdam, **1996**; b) M. E. Casida, D. P. Chong, *Recent Advances in Density Functional Methods*, vol. 1, World Scientific, Singapore, **1995**, p. 155.
[31] a) A. D. Becke, *J. Chem. Phys.* **1993**, *98*, 5648–5652; b) C. Lee, W. Yang, R. G. Parr, *Phys. Rev. B* **1988**, *37*, 785–789.
[32] For a review, see: A. Dreuw, M. Head-Gordon, *Chem. Rev.* **2005**, *105*, 4009–4037.
[33] For some recent examples, see: a) V. N. Nemykin, E. A. Makarova, J. O. Grosland, R. G. Hadt, A. Y. Koposov, *Inorg. Chem.* **2007**, *46*, 9591–9601; b) M. L. Lage, I. Fernández, M. J. Mancheño, M. A. Sierra, *Inorg. Chem.* **2008**, *47*, 5253–5258; c) H. Braunschweig, T. Herbst, D. Rais, S. Ghosh, T. Kupfer, K. Radacki, A. G. Crawford, R. W. Ward, T. B. Marder, I. Fernández, G. Frenking, *J. Am. Chem. Soc.* **2009**, *131*, 8989; d) M. L. Lage, I. Fernández, M. J. Mancheño, M. A. Sierra, *Chem. Eur. J.* **2010**, *16*, 6616–6624. For recent examples of B3LYP and TD-B3LYP calculations on push-pull systems, see: e) P. D. Jarowski, Y.-L. Wu, W. B. Schweizer, F. Diederich, *Org. Lett.* **2008**, *10*, 3347–3350, and ref. [2a] and [14b].
[34] a) *Modern Cyclophane Chemistry* (Eds.: R. Gleiter, H. Hopf), Wiley-VCH, Weinheim, Germany, **2004**; b) F. Diederich, *Cyclophanes*, Royal Society of Chemistry, Cambridge, UK, **1991**; c) *Cyclophanes* (Ed.: F. Vögtle), Springer, Heidelberg, Germany, **1983**.
[35] a) T. Moriguchi, K. Sakata, A. Tsuge, *J. Chem. Soc. Perkin Trans. 2* **2001**, 934–938; b) A. Tsuge, T. Nishimoto, T. Uchida, M. Yasutake, T. Moriguchi, K. Sakata, *J. Org. Chem.* **1999**, *64*, 7246–7248; c) T. Moriguchi, M. Yasutake, K. Sakata, A. Tsuge, *J. Chem. Res. Synop.* **1999**, 78–79; d) T. Moriguchi, K. Sakata, A. Tsuge, *J. Chem. Soc. Perkin Trans. 2* **1997**, 2141–2144; e) A. Tsuge, M. Yasutake, T. Moriguchi, K. Sakata, T. Yamato, S. Mataka, M. Tashiro, *Chem. Lett.* **1997**, 413–414; f) A. Tsuge, T. Moriguchi, S. Mataka, M. Tashiro, *Liebigs Ann.* **1996**, 769–771; g) A. Tsuge, T. Moriguchi, S. Mataka, M. Tashiro, *J. Chem. Soc. Perkin Trans. 1* **1993**, 2211–2215.
[36] For recent examples of transannular interactions in cyclophanes, see: a) L. M. Salonen, M. Ellermann, F. Diederich, *Angew. Chem. Int. Ed.* **2011**, *50*, 4808–4842; b) J. K. Klosterman, Y. Yamauchi, M. Fujita, *Chem. Soc. Rev.* **2009**, *38*, 1714–1725; c) M. Fujitsuka, S. Tojo, T. Shinmyozu, T. Majima, *Chem. Commun.* **2009**, 1553–1555; d) M. Shibahara, M. Watanabe, T. Iwanaga, T. Matsumoto, K. Ideta, T. Shinmyozu, *J. Org. Chem.* **2008**, *73*, 4433–4442; e) H. Hopf, *Angew. Chem.* **2008**, *120*, 9954; *Angew. Chem. Int. Ed.* **2008**, *47*, 9808–9812; f) G. F. Caramori, S. E. Galembeck, *J. Phys. Chem. A* **2007**, *111*, 1705–1712; g) J. W. Hong, H. Y. Woo, B. Liu, G. C. Bazan, *J. Am. Chem. Soc.* **2005**, *127*, 7435–7443; h) K. A. Lyssenko, M. Y. Antipin, D. Y. Antonov, *ChemPhysChem* **2003**, *4*, 817–823.
[37] a) L. Yu, H.-J. Schneider, *Eur. J. Org. Chem.* **1999**, 1619–1625; b) M. Mantina, A. C. Chamberlin, R. Valero, C. J. Cramer, D. G. Truhlar, *J. Phys. Chem. A* **2009**, *113*, 5806–5812.
[38] a) M. C. Etter, *J. Phys. Chem.* **1991**, *95*, 4601–4610; b) M. C. Etter, *Acc. Chem. Res.* **1990**, *23*, 120–126; c) T. W. Panunto, Z. Urbánczyk-Lipkowska, R. Johnson, M. C. Etter, *J. Am. Chem. Soc.* **1987**, *109*, 7786–7797.
[39] H.-H. Perkampus, *UV/Vis Atlas of Organic Compounds*, VCH Verlagsgesellschaft, Weinheim, Germany, **1992**.
[40] C. Hansch, A. Leo, R. W. Taft, *Chem. Rev.* **1991**, *91*, 165–195.
[41] a) H. Inoue, Y. Mikami, T. Yokotani, *Bull. Chem. Soc. Jpn.* **1973**, *46*, 3614–3615; b) W. N. White, *J. Am. Chem. Soc.* **1959**, *81*, 2912–2913.
[42] K. S. Thanthiriwatte, K. M. Nalin da Silva, *THEOCHEM* **2002**, *617*, 169–175, and references cited therein.

Received: February 9, 2012
Published Online: March 15, 2012

 © 2012 Wiley-VCH Verlag GmbH & Co. KGaA, Weinheim